AD-A193 076 PERCEPTION OF MOTION IN STATISTICALLY-DEFINED DISPLAYS 1/2
(U) NORTHWESTERN UNIV EVANSTON IL CRESAP NEUROSCIENCE
LAB R SEKULER 15 FEB 88 AFOSR-TR-88-0200 AFOSR-85-0370
UNCLASSIFIED F/G 5/8 NL

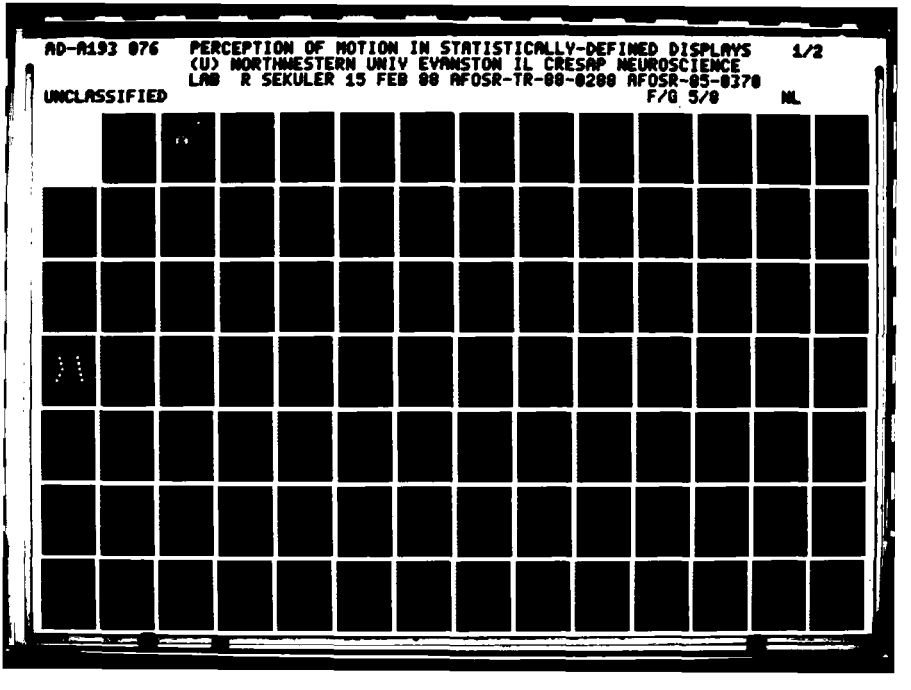

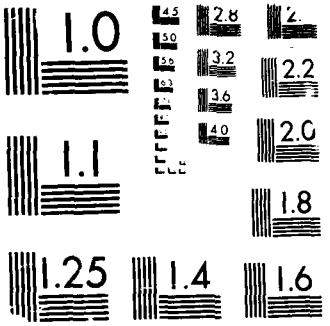

Report AFOSR-85-0370

Perception of Motion in Statistically-Defined Displays

Robert Sekuler
Cresap Laboratory
Northwestern University
Evanston IL 60201

15 February 1988

Annual Scientific Report for Period
1 October 1986 to 30 September 1987

Prepared for
Air Force Office of Scientific Research
Bolling Air Force Base, DC 20332

SECURITY CLASSIFICATION OF THIS PAGE

ADA193076

REPORT DOCUMENTATION PAGE

1a. REPORT SECURITY CLASSIFICATION: Unclassified	1b. RESTRICTIVE MARKINGS
2a. SECURITY CLASSIFICATION AUTHORITY	3. DISTRIBUTION/AVAILABILITY OF REPORT: Unlimited
2b. DECLASSIFICATION/DOWNGRADING SCHEDULE	
4. PERFORMING ORGANIZATION REPORT NUMBER(S)	5. MONITORING ORGANIZATION REPORT NUMBER(S): AFOSR-TR- 88-0288
6a. NAME OF PERFORMING ORGANIZATION: Northwestern University; 6b. OFFICE SYMBOL (If applicable)	7a. NAME OF MONITORING ORGANIZATION: Air Force Office of Scientific Research
6c. ADDRESS (City, State and ZIP Code): Cresap Neuroscience Laboratory, Evanston, Illinois 60208	7b. ADDRESS (City, State and ZIP Code): BLDG 410, Bolling Air Force Base, DC 20332-6448
8a. NAME OF FUNDING/SPONSORING ORGANIZATION: AFOSR; 8b. OFFICE SYMBOL (If applicable): NL	9. PROCUREMENT INSTRUMENT IDENTIFICATION NUMBER: AFOSR 85-0370
8c. ADDRESS (City, State and ZIP Code): BLDG 410, BAFB DC 20332-6448	10. SOURCE OF FUNDING NOS.

PROGRAM ELEMENT NO.	PROJECT NO.	TASK NO.	WORK UNIT NO.
61102F	2312	A5	

11. TITLE (Include Security Classification): Perception of Motion in Statistically-Defined Displays

12. PERSONAL AUTHOR(S): Sekuler, Robert

13a. TYPE OF REPORT	13b. TIME COVERED	14. DATE OF REPORT (Yr., Mo., Day)	15. PAGE COUNT
Annual Scientific	FROM 10-1-86 TO 9-29-87	2-15-88	98

16. SUPPLEMENTARY NOTATION

17. COSATI CODES			18. SUBJECT TERMS (Continue on reverse if necessary and identify by block number)
FIELD	GROUP	SUB. GR.	Vision, perception, motion, mathematical model, computational model, statistical displays, cinematograms

19. ABSTRACT (Continue on reverse if necessary and identify by block number)

Prior work on this project explored various aspects of motion perception using statistically complex displays. The project's aim has been to establish the characteristics of human visual mechanisms that are responsible for extracting information from such displays. During the present reporting period we have pursued two new dimensions of the general problem.

In the first subproject, we created random-dot cinematograms in which each dot's successive movements were independently drawn from a Gaussian distribution of directions of some characteristic bandwidth. Such a display, comprising many different, spatially intermingled local motion

20. DISTRIBUTION/AVAILABILITY OF ABSTRACT	21. ABSTRACT SECURITY CLASSIFICATION	
UNCLASSIFIED/UNLIMITED ☒ SAME AS RPT. ☐ DTIC USERS ☐		
22a. NAME OF RESPONSIBLE INDIVIDUAL: Dr Remy	22b. TELEPHONE NUMBER (Include Area Code): 202-767-4278	22c. OFFICE SYMBOL: NL

DD FORM 1473, 83 APR EDITION OF 1 JAN 73 IS OBSOLETE.

SECURITY CLASSIFICATION OF THIS PAGE

Block 19 (Continued)

vectors, can produce a percept of global coherent motion in a single direction. Using pairs of cinematograms, direction discrimination of global motion was measured under various conditions of direction distribution bandwidth, exposure duration, and constancy of each dot's path. A line-element model gave an excellent account of the results: i) over a considerable range, discrimination was unaffected by the cinematogram's direction distribution bandwidth; ii) only for the briefest presentations did changes in duration have an effect; iii) so long as the overall directional content of the cinematogram remained unchanged, the constancy or randomness of individual dots' paths did not affect discrimination. Finally, the line-element model continued to give a good account of the results when we made additional measurements with uniform rather than Gaussian distributions of directions.

Our second major research effort sought to identify the information that controlled speeded response to motion onset or change in motion. Observers were required to react to the change in movement of a random-dot field whose velocity switched abruptly from V_0 to V_1. Changes in velocity were created by either shifting the speed, with direction constant, or by reversing direction, with speed constant. Mean reaction times and their standard deviations were decreasing functions of the difference $|V_1-V_0|$, and increasing function of the initial speed, $|V_0|$. The results are quantitatively accounted for by a modification of the Local Dispersion model that Dzhafarov and Allik proposed for motion detectability. In our modification, detection of change of velocity from V_0 to V_1 is treated as structurally equivalent to the detection of onset of a motion whose velocity is $|V_1-V_0|$. We have found that the Local Dispersion model can be realized by the mass activation of network of bilocal correlators.

Report AFOSR-85-0370

Perception of Motion in Statistically-Defined Displays

Robert Sekuler
Cresap Laboratory
Northwestern University
Evanston IL 60201

15 February 1988

Annual Scientific Report for Period
1 October 1986 to 30 September 1987

Prepared for
Air Force Office of Scientific Research
Bolling Air Force Base, DC 20332

Written Publications in Technical Journals

Ball, K., and Sekuler, R. Direction-specific improvement in motion discrimination. Vision Research 1987 *27* 953-965.

Williams, D., and Phillips, G. Cooperative phenomena in the perception of motion direction. Journal of the Optical Society of America A *4* 878-885.

Sekuler, R., Anstis, S., Braddick. O.J., Brandt, T., Movshon, A.J., and Orban, G. (in preparation) Motion perception: psychophysics and cortical physiology. In L. Spillman and J.S. Werner (editors) The Neurophysiological Foundations of Visual Perception. Academic Press, New York.

Dzhafarov, E., Sekuler, R., Allik, J., and Williams, D. Reaction times to change in speed and direction of motion. Submitted to Journal of experimental Psychology: Human Perception and Performance

Watamaniuk, S.N.J., Sekuler, R., and Williams, D. Direction perception in complex dynamic displays: Integration of direction information. Submitted to Vision Research.

Professional Personnel Associated with Research Effort

Robert Sekuler, Ph.D.
Douglas Williams, Ph.D.
Scott Watamaniuk, M.A.
Ehtibar Dzhafarov, Ph.D.
Mark Nawrot, B.A.

Interactions by Principal Investigator.

The richness of motion perception. Lecture to Brain and Information Sciences Group, Massachusetts Institute of Technology, March 1987

Motion perception, Badenweiler Conference on Neurophysiological Foundations of Visual Perception, Badenweiler, West Germany, August 1987.

Project One:

Direction Perception in Complex Dynamic Displays: The Integration of Direction Information

Scott Watamaniuk, Robert Sekuler
and Douglas W. Williams

INTRODUCTION

Though motion perception does depend upon spatially local processes, under certain circumstances global processes make an important contribution. For example, the human visual system can integrate different, spatially-intermingled motion vectors into a global percept of motion in a single direction (Adelson and Movshon, 1982; Williams and Sekuler, 1984). Such integrated percepts may offer important clues to the mechanisms of motion perception. To exploit such clues we have followed the tradition of using discrimination performance to probe underlying psychophysical mechanisms (e.g., Graham, 1965; Wilson and Gelb, 1984). Specifically, we were interested in how easily observers could discriminate between two different global motions when each had resulted from the integration of many different motion vectors.

Our stimuli were random dot cinematograms in which each dot took an independent two-dimensional random walk with steps of constant size. The direction any dot moved, from one display frame to the next, was independent of the dot's previous movements as well as the movements of other dots. All dots chose their directions of movement from the same probability distribution. Williams and Sekuler (1984), using uniform distributions of directions, showed that the resulting global percept of motion depends upon the range of the distribution. Specifically, uniform distributions with ranges of directions less than 180° tend to produce a perception of global motion in the approximate direction of the distribution's

mean even though the random perturbations of each dot are evident. As the range increases further, the perception of global motion diminishes, until at the limit, a uniform distribution with 360° yields a percept of only local random motion of individual dots. In this present study, we measured the discriminability of the direction of global motion using Gaussian distributions of directions.

To anticipate, our results show that direction discrimination of the global motion percept is influenced by both the bandwidth of the controlling direction distribution and duration of the stimuli, but not by the paths travelled by individual dots over time. As will be shown later in the discussion, our data are consistent with a line-element model described previously by Williams et al. (1984).

METHODS

Stimuli

Stimuli were 256 computer-generated dots plotted on a cathode ray tube (CRT) display with a relatively fast, P4, phosphor. A mask, with a circular aperture 8° in diameter, covered the face of the CRT. This aperture allowed only about 130 of the 256 dots to be visible at any one time. The density of dots was 2.56 dots per square degree of visual angle. Each dot subtended 6'. Luminance of a single dot was about 0.82 cd/m^2. The luminance of the mask was 0.07 cd/m2; the veiling luminance was 0.03 cd/m^2.

Stimuli were presented at a frame rate of 17.5 Hz. From frame to frame, each dot's movements were controlled by a predefined distribution of directions stored as an array of x- and y-increments. The predefined distribution of directions chosen was

Gaussian.[1] The computer read the increment values for a dot's movements from the array, added the increments to the dot's current position and transmitted the dot's new x- and y-position to the CRT display via digital-to-analog converters. The initial screen location of each dot was randomized for each presentation, rendering the pattern of dots an unreliable clue to direction.

Supported and restrained by a chin-headrest, the seated observer viewed the CRT monocularly from a distance of 57 cm. The non-preferred eye was covered by a translucent patch. The height of the CRT was set so that the center of the aperture was at approximately eye level and observers were required to maintain fixation on a dot located at the center of the aperture. Push-buttons connected to the computer initiated each trial and signalled the observer's responses.

Observers

One of the authors (SW) and four university students served as observers for all experiments. Except for SW, all observers were naive to the purposes of the present experiments and had normal, or corrected-to-normal, visual acuity. Those who required corrective lenses wore them for all experiments.

Procedure

Stimuli were presented in a two-alternative forced-choice procedure. Though the durations of the paired test intervals varied from condition to condition, on any single trial the two were always of equal duration. Interstimulus interval was fixed at 500 msec.

Different distributions of directions governed motion in the

two intervals of each trial. One test interval, picked at random, was governed by a distribution whose mean direction was 90 deg (upwards); we'll refer to this stimulus as the standard. Motion in the other test interval was governed by a distribution whose mean was greater than 90 deg (that is, counterclockwise of upwards); we'll refer to this stimulus as the comparison. The observer had to identify the interval in which the global direction of motion was upwards.

A session consisted of six blocks, 48 trials each. A block of trials was characterized by one combination of direction bandwidth and test-interval duration. In order to produce a large range of discrimination performance, from chance to near perfection, six comparison stimuli with different mean directions were used in each block. Trial-wise feedback was provided, with a low tone signalling an incorrect response. Approximately four seconds elapsed between trials. Over any 48-trial block, the standard stimulus appeared equally often in the first and second intervals.

EXPERIMENTS

Experiment I. Bandwidth and Duration

This experiment examined direction discrimination as a function of i)the directions present in the stimulus, and ii)stimulus duration. Four ranges of directions were used, each defined by a different Gaussian distribution of directions. The distributions had standard deviations (SD) of 0.0,[2] 17, 34, and 51 deg. Larger standard deviations, or bandwidths, imply a greater range of directions was simultaneously present in the cinematogram. All standard deviations used produced global motion in the approximate

direction of the mean of the distribution.

A pilot study showed that discrimination varied with bandwidth. So, to span the psychometric functions of each bandwidth, sets of comparison stimuli with different means were needed. Table 1 lists the six comparison means associated with each bandwidth. Five durations of presentation, three, six, nine, 12, and 25 frames, were completely crossed with the four bandwidths. For each combination of bandwidth and duration, an observer was tested on a total of 288 trials.

Table 1 about here

Analysis

Responses were aggregated to yield the percent correct for each combination of standard and comparison. The percent correct responses for individual observers were then fit by the Quick (1974) psychometric function, given by

$$\Psi(S)=1-2^{-(k*S)^P} \qquad [1]$$

where S is the separation in mean direction between the standard and comparison stimulus, measured in deg, $1/k$ is the difference between standard and comparison means at which $\Psi(S)$ equals 0.5 (chance performance), and P determines the maximum slope of the function in the neighborhood of 75% correct. This function provided good fits to the observed data (mean r^2 for 100 data sets was 0.89). Discrimination thresholds, defined as the difference between standard and comparison mean directions sufficient to yield 75%

correct, were evaluated from the fitted psychometric functions. Threshold values were then treated by analysis of variance (ANOVA) including a trend analysis on the two variables.[3]

RESULTS

Discrimination thresholds, averaged over observers, are plotted as a function of bandwidth in Figure 1. As the figure shows, discrimination thresholds for each duration increased with stimulus bandwidth. Generally, discrimination thresholds changed relatively little as stimulus SD was increased from 0.0 to 17 degrees, but changed substantially with further increases. This observation was confirmed with a trend analysis of the data averaged over durations, which yielded significant linear and non-linear components ($F_{1,2}$ = 5520.72 and $F_{2,4}$ = 8.45, both $P<0.05$). Notice that at the smallest bandwidths, the discrimination thresholds for the four longest durations are indistinguishable. However divergence does occur as bandwidth gets larger. In contrast, the results at the shortest duration, three frames, differ from those of other durations at all bandwidths. This interaction between bandwidth and duration was confirmed by the ANOVA ($F_{12,24}$ = 13.03, $P<.05$). This implies that as bandwidth grows, it may take longer to perceive the global flow. It is clear however, that regardless of bandwidth, discrimination thresholds obtained with the briefest presentations are consistently higher than those obtained with longer ones.

Figure 1 about here

To more clearly show the effect of duration, we have replotted

the data as a function of duration in Figure 2. The figure shows a progressive decrease in discrimination threshold as a function of duration (linear trend $F_{1,2} = 256.74$, $P<0.05$). However, the decrease in threshold with duration also contains non-linear components ($F_{3,6} = 14.72$, $P<0.05$). A larger decrease occurred when duration was increased from three to six frames than when duration was increased from 12 to 25 frames. Moreover, discrimination thresholds for the two smallest bandwidths seemed to reach an asymptotic level between six and 25 frames of duration. In contrast, for the largest bandwidth, each increase in duration produced a further decrease in the discrimination threshold.

Figure 2 about here

Experiment II. Effective Dot Path

In Experiment I, discrimination thresholds increased as bandwidth increased. However, because several aspects of the stimuli covary with bandwidth, that experiment does not allow unequivocal inferences to be made about the cause of the threshold increase. By definition, the number of directions contained in a stimulus increases with bandwidth. So, as bandwidth increases, the path taken by any single dot contains a greater variety of directions. This greater variety might itself have increased the variability of the perceived global direction, thereby impairing global direction discrimination for the stimulus as a whole. We wanted to determine, therefore, how discrimination performance might vary with the number of directions occurring in each dot's path.

To answer this question, we created two stimuli that produced

very different individual dot paths but had the same aggregate direction distribution. Both types of stimuli are illustrated in Figure 3. In one, dots took a two-dimensional random walk as described earlier. Because each dot's path was random, within limits imposed by the distribution bandwidth, we'll refer to such a stimulus as the random-path type. Such paths are represented in panel A for two different dots. In the other type of stimulus, a different scheme generated a dot's path. Once a dot had randomly chosen a direction for its first displacement, it continued to move in that same direction for the entire presentation. Because each dot moved along its own characteristic fixed path, we'll refer to such a stimulus as the fixed-path type. Such paths are represented in panel B for two different dots. Note that although the aggregate direction distributions for both stimuli are identical, the variability of their dot paths are very different. In the random-path stimulus, the controlling distribution of directions creates differences between different dots' paths, and also introduces randomness to any single dot's path. In the fixed-path stimulus, the controlling distribution affects only differences between different dots' paths.

Figure 3 about here

The two stimulus types were used to produce three test conditions. In one condition, both presentations within a single trial were fixed-path stimuli (fixed-path condition). In a second condition, both presentations were random-path stimuli (random-path condition). In the third condition, one random-path and one fixed-

path stimulus were presented on each trial (combined condition). In this last condition, the two types of motion were completely crossed with respect to which served as the standard or comparison and also their presentation order.

Discrimination performance was measured for six separations between the standard and comparison mean directions: 2, 4, 5, 6, 8, and 10 deg. All stimuli had a Gaussian direction distribution with a standard deviation of 34 deg. Each stimulus was presented for nine frames. This bandwidth and duration were chosen because in previous experiments this combination produced a moderate level of performance. This ensured some latitude for discrimination performance to improve or grow poorer as condition varied from random-path to fixed-path. Observers were the same as those in Experiment I.

RESULTS

The data, averaged over observers and represented as percent correct, are plotted as a function of the difference in mean direction between the standard and comparison stimuli in Figure 4A. The figure shows that all three conditions yielded similar discrimination ($F_{2,8} = 1.22$, $P>.05$).

Figure 4 about here

At the duration used in this experiment, nine frames, the two types of motion were different. However, if one looked at the stimuli through a narrow time window, in particular, examining only a single pair of successive frames, the minimum needed to define motion, the two types of stimuli would be indistinguishable. We

were concerned, therefore, that this short-term similarity between stimuli might account for the similarity in performance with the two types of motion. This concern would be serious if performance had become asymptotic at a presentation of just two frames. Then, observers would have extracted all the necessary stimulus information before any real differences between stimulus types could have become manifest. But for our experiments this concern is not justified.

Results from Experiment I show that asymptotic performance in Experiment II would certainly have required presentations longer than just two frames. In Figure 4B we have plotted the average of the earlier results for the stimulus with an SD of 34 degrees presented for three frames, the shortest presentation used. The averaged results from the present experiment, for both stimulus types, are also plotted in that figure. Recall that all cinematograms in that earlier experiment were of the type we've labelled "random path". Note that performance with presentations of only three frames in Experiment I was far below that obtained in Experiment II, with nine frames. Therefore, within just two frames, observers in Experiment II had not extracted all the necessary information to determine the direction of motion. So, the identity of random-path and constant-path stimuli over the first two frames of presentation cannot explain the lack of performance difference between the stimuli at nine frames.

The results of Experiment II suggest that individual dot paths over frames are not being used by the visual system in determining the direction of global perceived motion. Rather, perceived global direction seems to depend only upon the <u>distribution</u> of directions of motion present from one frame to the next. That is, the visual

system keeps track of the directions created by any one displacement but does not keep track of the successive movements, over frames, of individual dots.

DISCUSSION

As stated earlier, one of the major objectives of this research is to account for our results with a line-element model of direction discrimination. Before discussing the model, it will be useful to relate our results to those in the literature and discuss the implications that these results hold for research in motion perception.

We have found that direction discrimination of random-dot cinematograms depends upon certain stimulus dimensions. First, increasing stimulus bandwidth decreases direction discrimination. Further, increasing stimulus duration results in an improvement in discrimination performance. However, in developing its representation of global direction, the visual system appears to disregard information about individual dot paths over time.

Williams and Sekuler (1984), using stimuli similar to that used here, found that global motion in a single direction was always seen when the range of the uniform direction distribution was less than or equal to 180 deg. Experiment I showed that, although unidirectional global motion was always perceived, as the bandwidth of the direction distribution increased so did the discrimination threshold. The present results suggest that although coherent global flow can be created by any one of a wide range of bandwidths, the precise direction seen may not be as predictable. In other words, the directional bandwidth controls the precision with which the perceived direction matches the mean of the direction distribu-

tion.

Experiment I also provided some indication of the integrative power of the visual system in determining direction of motion. Figure 1 showed that direction discrimination did not change significantly when the bandwidth of the stimulus was raised from SD=0.0 to SD=17 deg. This occurred even though the two distributions produced highly distinguishable patterns of movement. The visual system seems to extract and integrate directional information just as easily from stimuli containing many different directions (the stimulus with an SD of 17 deg contained 79 different directions of motion) as it does with only a single direction present.

But bandwidth was not the only variable that influenced discrimination. Stimulus duration also had an impact: as the duration of the stimuli increased, direction discrimination improved. This implies some sort of temporal summation in the process that governs perceived direction of motion. Note that the number of frames needed to reach asymptotic performance is not the same for all bandwidths: as bandwidth decreases, fewer frames are needed to produce asymptotic performance.

Experiment II examined the effect of dot path on discrimination. The results showed that when direction distributions were identical, whether the dots took random walks or followed fixed but different paths, discrimination was unchanged. Previously, Williams and Sekuler (1984) showed that the global percept of motion does not depend on the spatial relationship between local motion vectors over time. Our findings agree with this view: when many vectors of motion are present, the direction of global motion is determined by the <u>distribution</u> of directions rather than by the individual dot

paths.

This result also has some methodological, as well as theoretical, implications. Some researchers, utilizing random dot displays, have purposely limited the lifespan of individual dots to restrict the directional information contained within a single dot path (e.g. Mather and Moulden, 1980; Mather and Moulden, 1983). The present result, that individual dot paths do not affect direction discrimination, suggests that this control may not always be necessary. When the stimulus is comprised of many random dots, the visual system does not necessarily utilize information about the consecutive movements of individual dots.

THEORY

A Line-Element Model of Direction Discrimination

As stated earlier, one of our objectives was to account for global direction discrimination with a line-element model. Line-element models have been successful in accounting for several visual discrimination tasks involving dimensions such as wavelength and spatial-frequency (Graham, 1965; Wilson and Gelb, 1984; Wilson and Regan, 1984; Wilson, 1985). A line-element model has also been useful for predicting the conditions under which random dot displays with very different direction distributions would be metameric, that is indistinguishable perceptually despite their considerable physical differences (Williams et al., 1984).

Any line-element model has three defining characteristics. First, it postulates mechanisms whose sensitivity profiles span the stimulus dimension of interest. For any stimulus, the total response of a mechanism is the sum of that mechanism's individual responses to each component of the stimulus. Second, discrimination

between two stimuli depends upon the change in a mechanism's response as a result of a change in stimulus components. Finally, the differences in responses to two stimuli are pooled over all mechanisms. This implies that the discriminability of two stimuli is a function of a scalar value (Graham, 1965).

An example of a line-element model is one Williams et al. (1984) used to predict which set of discrete directions of motion would have to be mixed in order to generate a percept that was indistinguishable from one generated by a stimulus containing a broad band of directions of motion. This model comprised a set of direction selective mechanisms, and the response of the model depended only upon the component directions of the stimulus. Based on the success of this line-element model and the demonstration that direction discrimination depends only upon the distribution of directions, it seemed reasonable to attempt to fit the present data with the same model.

In the remainder of the discussion, we will describe the basic structure of the line-element model that we used to account for the present data. Parameters of the model will be estimated using data obtained for stimuli with Gaussian distributions of directions presented for 12 frames. The same parameters will then be used to account data obtained with different presentation durations and predict results for stimuli that had uniform, rather than Gaussian, direction distributions.

Description of the Model

The basic structure and assumptions of the present model are are the same as those used to account for motion metamers (Williams et al., 1984). The present model assumes that the full range of

directions (360^{o}) is spanned by a small number of evenly-spaced, bandlimited, directionally-selective mechanisms. All mechanisms have the same Gaussian profile; center-to-center separation between any two adjacent mechanisms is equal to the half-amplitude half-bandwidth of a mechanism.

The sensitivity of the i^{th} mechanism, centered at θ_i, to direction of motion θ is given by

$$S_i(\theta) = \exp^{\{-[(\theta-\theta_i)/h]^2 * \ln 2\}} \qquad [2]$$

where h is the half-amplitude half-bandwidth of the mechanism. The response of the i^{th} mechanism to a distribution of directions, $D(\theta)$, is given by

$$R_i(D) = \sum_{\theta=1}^{360} S_i(\theta) * pr\{D(\theta)\}, \qquad [3]$$

where $S_i(\theta)$ is the i^{th} mechanism's sensitivity to direction θ, and $pr\{D(\theta)\}$ is the proportion of dots in distribution $D(\theta)$ that move in direction θ.

To predict the discriminability of any two distributions, $D(\theta_1)$ and $D(\theta_2)$, with different mean directions, one calculates the difference, for each mechanism, between its responses to the two distributions

$$\Delta R_i = R_i\{D(\theta_1)\} - R_i\{D(\theta_2)\}. \qquad [4]$$

These differences are then pooled for all the individual mechanisms

according to a Q^{th} norm rule:

$$\Delta R = \{\sum_{i=1}^{M} |\Delta R_i|^Q\}^{1/Q}, \qquad [5]$$

where M is the number of mechanisms. ΔR represents the total difference between the responses to the two stimuli generated within the visual system. Note that this method of pooling allows for the effects of probability summation (Quick,1974).

The variable Q determines the way response differences, ΔR_i, for each mechanism will be combined. If Q=1, all ΔR_i's are weighted equally and the system would be taking the simple sum of all ΔR_i's. If Q>1, the larger values of ΔR_i are weighted more heavily than smaller values; if Q=infinity, the model acts as a peak detector, taking only the single largest value of ΔR_i into account.

In order to relate the predicted values of ΔR to the data obtained in Experiment I, we used a psychometric function of the form:

$$Y(\Delta R) = 1 - 2^{-(k*\Delta R)^P} \qquad [6]$$

where k is equal to the value of $1/\Delta R$ at $Y(\Delta R)=0.50$ and P is related to the slope of the psychometric function.

The model as described above has four free parameters, two of which we fixed on <u>a priori</u> grounds. Previous researchers, Wilson and Gelb (1984), have shown that when Q=2, a line-element model provides good fits to spatial-frequency discrimination data when the stimuli are presented under <u>sustained</u> temporal conditions. The

temporal modulation of their sustained stimulus was Gaussian with a 1/e time constant of about 250 msec. Following Wilson and Gelb, we decided to use Q=2 in order to fit the data we obtained at a duration of 12 frames, since at this duration, thresholds for the three smallest standard deviations first reached asymptotic levels. This decision left three free parameters, k, P, and M, the number of mechanisms.

We set M=12 in accordance with Williams et al. (1984) who found that a model with 12 mechanisms accounted for metameric relations between cinematograms that contained a wide range of directions and cinematograms that contained just a few directions. Having fixed Q and M, we estimated the optimum values for k and P by a least-mean-squares fit to Experiment I data presented for 12 frames. Table 2 shows the chi-square (χ^2) goodness-of-fit values obtained for best-fits to the present data. All χ^2 values are well below the critical value suggesting that the model fit the data well.

Table 2 about here

Model Fits for Various Durations

The model as described above, provided a satisfactory account of data obtained for stimuli presented for a long duration, 12 frames, with Q=2. Since the six-, nine-, 12-, and 25-frame conditions seemed to be grouped together (see Figure 1), the same parameters used to fit the 12-frame data were also used to fit the six-, nine-, and 25-frame data. The predicted values along with the observed data for the six-frame condition, for all observers, are presented in Figure 5. Those for the nine-frame condition appear in

Figure 6 while those for the 25-frame condition appear in Figure 7. Data are shown by the filled squares and the model by the lines. For all three duration conditions, the model captures the trend of the data. Chi-square goodness-of-fit values for the six-, nine-, and 25-frame data appear in Table 3. The χ^2 values for all observers were below the critical value.

Figure 5, 6, and 7 about here

Table 3 about here

Discrimination thresholds obtained at durations of six frames or greater appear to be grouped together (see Figure 1). However, for the shortest presentation, three frames, discrimination was poorer. Since a model of direction discrimination should account for this effect of duration, we sought to use the present model to predict discrimination for this very short stimulus duration.

Previously, Wilson and Gelb (1984) demonstrated an empirical relation between Q and stimulus duration. They found that a line-element model with Q=2 predicted spatial-frequency discrimination when the stimuli were presented in sustained temporal conditions. When the stimulus was only presented for about 125 msec (transient condition), Q=2 did not give a good account of the data, but Q=6 did. Since the duration of three frames, in msec, was close to that of the transient condition described by Wilson and Gelb, we used Q=6 to predict discrimination in the three-frame condition. The values of k, M, and P remained fixed at the values previously estimated.

Figure 8 compares the model fits to the three-frame data for all observers, measured for various stimulus standard deviations.

Data are represented by filled squares and the model calculations by the lines. Across any row, all the graphs show data for a single standard deviation; within any column, graphs are for a single observer. Table 3 lists the χ^2 values for each observer. Since there were four standard deviations crossed with six separations, there were a total of 24 data points per person used in the calculation of χ^2. As can be seen, all but one of the χ^2 values are below the critical value. Inspection of Figure 8 shows that although the general trend of the data is captured by the model, the fits are not particularly good for the largest standard deviation. The fits would not have been appreciably improved by increasing Q beyond its set value of six since predictions change little as Q is raised above this value. This relatively poor fit to the data can not be reconciled at this time.

Figure 8 about here

Discrimination with Uniform Distributions

We next sought to determine whether the model parameters developed for long-duration stimuli with Gaussian direction distributions (Experiment I) could also account for performance with a different distribution of directions. So we measured direction discrimination, for the same observers as before, now using stimuli with uniform direction distributions. The uniform distributions had ranges of 1, 31, 91, and 161 deg. As we did earlier with the Gaussian stimuli, discrimination was measured for six separations between mean directions, yielding 24 data points per person (separation values for each uniform distribution are found in Table 1).

All stimuli were presented for 12 frames.

Figure 9 compares the predictions of the 12-mechanism model to data obtained with the four uniform stimuli for all observers. This is a parameter free fit to the data, the parameters having been determined in fitting the model to the long-duration Gaussian data. Data are represented by the filled squares and predictions by the lines. Inspection of the figure shows that qualitatively, the model captures the trends in the observed data well. Chi-square goodness-of-fit values were evaluated, for each observer, using all 24 points obtained with the uniform stimuli. The χ^2 values for each observer for the fitted data (Gaussian stimuli) and predicted data (uniform stimuli) are found in Table 2. For all observers, the χ^2 values were well below the critical value. Thus the same parameters that earlier gave a good account of data with long-duration Gaussian stimuli, also give a good account of data with long-duration uniform stimuli.

Figure 9 about here

Summary of Model Results

For all observers, a line-element model with 12 mechanisms and Q=2, provided a good fit to data obtained with Gaussian direction distributions presented for 12 frames. Consistent with the idea that durations of six frames or greater fall into the same group (see Figure 1), the same parameters that provided good fits for the 12-frame data also provided good fits for the six-, nine-, and 25-frame data. For the briefest stimuli, three frames, the model

required that Q=6. Finally, the same parameter set estimated for Gaussian direction distributions, presented for 12 frames, did a good job of predicting discrimination with four uniform distributions, presented for 12 frames.

Further Research

This research raises further questions about the ability of the visual system to integrate direction information. Although we have considered discrimination obtained with durations of six frames or greater as a group, it is apparent that for stimuli with large bandwidths there is a systematic change in discrimination with duration (see Figure 1). The present model, though adequate as a first approximation of the integration process, does not account for this bandwidth-duration interaction. Further research is needed to refine the model to account for this effect.

One aspect that has not been touched on here is the integration of information between the two eyes. In the present experiments, all stimuli were presented monocularly. An experiment that could help establish the locus of the integration would be to present part of the distribution of directions to each eye and measure the perceived direction of motion. By varying the relative proportion of the overall distribution shown to each eye and its directional content, we could establish how the visual system integrates motion information between the two eyes and how dissimilar the two stimuli must be before the integration system fails and rivalry results.

Another qu tion of interest is whether color has an effect on the integration of direction information. Recent physiological research has shown that the cells in the Medial Temporal area (MT), which are particularly responsive to complex moving stimuli (Newsome

et al. 1986), seem little influenced by color (Livingstone and Hubel, 1987). If MT neurons were involved in the detection and integration of direction information, then one could psychophysically test whether the color of the components of the moving stimuli affect the perceived direction of motion.

A final question concerns the power of the system to integrate various directions. In particular, how similar must component directions of a stimulus be in order for integration to occur? We have shown that people can discriminate the global direction of motion produced by a distribution of directions, with a high degree of accuracy, even when the bandwidth is quite large. However, we also know that if two very different directions of motion are presented simultaneously, the observer perceives both directions of motion but with the separation between them exaggerated (Marshak and Sekuler, 1979). Stimuli similar to ours could be used to examine the continuum between perceiving a single global direction of motion (integration) and simultaneously perceiving several different separate directions of motion (segregation). To explore this continuum, one could present stimuli containing many different directions, sampled at various spacings, and measure whether observers perceived a single global direction.

CONCLUSIONS

To summarize the findings and implications of the present studies: Increasing stimulus bandwidth decreases direction discrimination. Increasing stimulus duration results in an improvement in discrimination performance. In developing its representation of global direction, the visual system appears to disregard information

about individual dot paths. A line-element model with 12 mechanisms accounts for direction discrimination for a wide variety of stimulus bandwidths and durations. The model required a systematic change in Q, the parameter that reflects the mode of pooling across mechanisms, to account for the change in discrimination with duration. A Q of 6 was required for the shortest duration while a Q of 2 was required for longer durations. A possible mechanistic way to interpret the change in Q with duration is that as duration decreases, fewer of the mechanisms' responses enter into the pooled, overall response.

Acknowledgment-- This research was supported by a grant from the U.S. Air Force Office of Scientific Research, AFOSR 85-0370.

REFERENCES

Adelson, E. H. and Movshon, J. A. (1982) Phenomenal coherence of moving gratings, Nature, 300, 523-525.

Graham, C. H. (1965) Color: data and theories. In Vision and Visual Perception (C.H. Graham, et al. ed.), pp.414-451, Wiley, New York.

Livingstone, M. and Hubel, D. (1987) Psychophysical evidence for separate channels for the perception of form, color, movement, and depth. Journal of Neuroscience 7, 3416-3468.

Mather, G. and Moulden, B. (1980) A simultaneous shift in apparent direction: further evidence for a "distribution shift" model of direction coding. Quarterly Journal of Experimental Psychology 32, 325-333.

Marshak, W. and Sekuler, R. (1979) Mutual repulsion between moving visual targets. Science 205, 1399-1401.

Mather, G. and Moulden, B. (1983) Thresholds for movement direction: two directions are less detectable than one. Quarterly Journal of Experimental Psychology 35, 513-518.

Newsome, W., Mikami, A., and Wurtz, R. (1986) Motion selectivity in macaque visual cortex. III. psychophysics and physiology of apparent motion. Journal of Neurophysiology 55, 1340-1351.

Quick, R. F. (1974) A vector-magnitude model for contrast detection. Kybernetik 16, 65-67.

Williams, D. W. and Sekuler, R. (1984) Coherent global motion percepts from stochastic local motions. Vision Research 24, 55-62.

Williams, D. W., Tweten, S., and Sekuler, R. (1984) Using metamers to explore motion perception. Supplement to Investigative Ophthalmology and Visual Science 25, 14.

Wilson, H. R. (1985) Discrimination of contour curvature: data and theory. Journal of the Optical Society of America A 2, 1191-1198.

Wilson, H. R. and Gelb, D. J. (1984) Modified line-element theory for spatial-frequency and width discrimination. Journal of the Optical Society of America A 1, 124-131.

Wilson, H. R. and Regan, D. (1984) Spatial-frequency adaptation and grating discrimination: predictions of a line-element model. Journal of the Optical Society of America A 1, 1091-1096.

FIGURE CAPTIONS

Fig.1 Discrimination thresholds (see text for definition) for five durations, averaged over observers, plotted as a function of stimulus distribution standard deviation (SD). Notice that at all SDs, the three-frame thresholds are higher than all others. At the two smallest stimulus SDs, thresholds are identical for durations of six frames or more. For these same durations, thresholds diverge at larger SDs. At the two largest SDs, there seems to be a systematic change in thresholds with duration; thresholds decrease as duration increases.

Fig.2 Discrimination thresholds (see text for definition) for four stimulus distribution standard deviations, averaged over observers, plotted as a function of duration. Note that for the two smallest distribution SDs (filled and unfilled squares), thresholds have reached an asymptotic minimum after a duration of only six frames.

Fig.3 Two types of individual dot motion, random-path (A) and fixed-path (B). Note that only two directions of local motion are present in both A and B and that the vector-sum of the directions is the same in both cases.

Fig.4 Percent correct judgments as a function of mean direction separation. Data are averaged over all observers. (A) Data are presented for three dot-path conditions. Average standard error bars are provided in the legend for each condition. Notice that the three different conditions yield quite similar results. (B) Data, averaged

over the three dot-path conditions, are presented with data from Experiment I. These Experiment I data were obtained using the same stimulus bandwidth but presented for only three frames. Standard error bars are provided on each curve. Note that the three-frame data from Experiment I are far below the averaged data from Experiment II .

Fig.5 Data for four stimuli with Gaussian distributions of directions with different standard deviations (SD), presented for a duration of six frames. Data are represented by the filled squares while the solid curves represent fits from a 12-mechanism line-element model with Q=2. Each row of graphs represents data for a single stimulus distribution SD; each column provides a single observer's data. Note that the slope of the data gets shallower as the distribution SD increases and that the model fits follow this trend of the data.

Fig.6 As in Figure 5, but for a duration of nine frames.

Fig.7 As in Figure 5, but for a duration of 25 frames.

Fig.8 Data for four stimuli with Gaussian distributions of directions with different standard deviations (SD), presented for a duration of three frames. Data are represented by the filled squares while the solid curves represent fits from a 12-mechanism line-element model with Q=6.

Fig.9 Data for four bandwidths of uniform stimuli presented for 12 frames. Data are represented by the filled squares while the solid

curves represent predictions from a 12-mechanism line-element model with Q=2. Model parameters were evaluated from fitting data obtained for four stimuli with different Gaussian distribution standard deviations presented for 12 frames. Each row of graphs represents data for a single stimulus bandwidth; each column provides a single observer's data. As in the previous figures, the slope of the data gets shallower as the bandwidth increases; this trend is captured well by the model predictions.

Footnotes

1. Because of the discrete nature of the display, it was not possible to present a continuum of directions. We approximated a Gaussian distribution by sampling a one degree intervals.

2. The Gaussian distribution with a standard deviation of 0.0 deg signifies motion in which all dots moved in parallel paths in the same direction.

3. The evaluation of discrimination thresholds produced two extremely large values that were substantially different from the others. These extreme values were due to a lack of monotonicity in two observers' data for a particular bandwidth-duration combination. These two values were excluded from the ANOVA conducted on the bandwidth and duration data.

Table 1. Bandwidths and mean directions of stimuli with Gaussian and uniform direction distributions.

Standard Deviations of Gaussian Distributions	Mean Directions	
	Standard	Comparison
0.0 deg (unitary motion)	90 deg (upwards)	91, 92, 93, 94, 95, 96
17 deg	90 deg	91, 92, 94, 95, 96, 98
34 deg	90 deg	92, 94, 95, 96, 98, 100
51 deg	90 deg	92, 95, 97, 99, 102, 105

Ranges of Uniform Distributions	Mean Directions	
	Standard	Comparison
1 deg (unitary motion)	90 deg (upwards)	91, 92, 93, 94, 95, 96
31 deg	90 deg	91, 92, 93, 94, 95, 96
91 deg	90 deg	91, 92, 93, 96, 99, 102
161 deg	90 deg	92, 94, 95, 100, 105, 110

Table 2. Chi-square values of model fits to four Gaussian stimuli and predictions for four uniform stimuli presented for 12 frames.

Observer	Gaussian Distribution	Uniform Distribution
CC	8.35	24.92
CP	7.73	9.21
DA	4.88	7.63
JW	12.93	17.38
SW	4.16	5.60
critical $\chi^2_{.95}$	33.9 (df=22)	36.4 (df=24)

Note: Values underlined exceed critical χ^2.

Table 3. Chi-square values of model fits to four Gaussian stimuli presented for durations of three, six, nine, and 25 frames.

Observer	3 frames	6 frames	9 frames	25 frames
CC	27.62	12.93	11.35	13.03
CP	18.47	10.72	5.15	10.65
DA	24.00	14.66	7.03	5.78
JW	<u>50.17</u>	19.10	7.78	23.40
SW	18.47	15.64	8.35	3.87
critical $\chi^2_{.95}$	35.2 (df=23)	36.4 (df=24)	36.4 (df=24)	36.4 (df=24)

Note: Values <u>underlined</u> exceed critical χ^2.

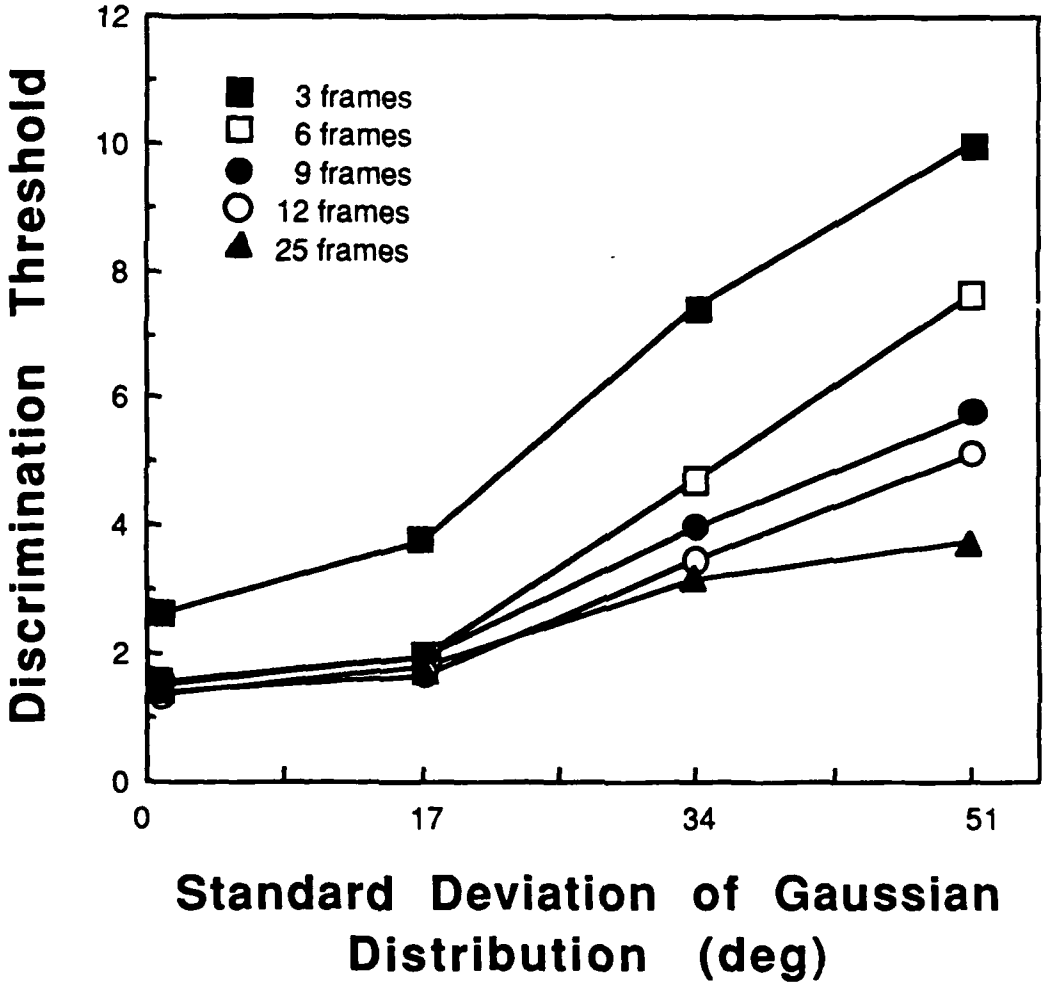
Discrimination Threshold
12
10
8
6
4
2
0
3 frames
6 frames
9 frames
12 frames
25 frames
0
17
34
51
Standard Deviation of Gaussian Distribution (deg)

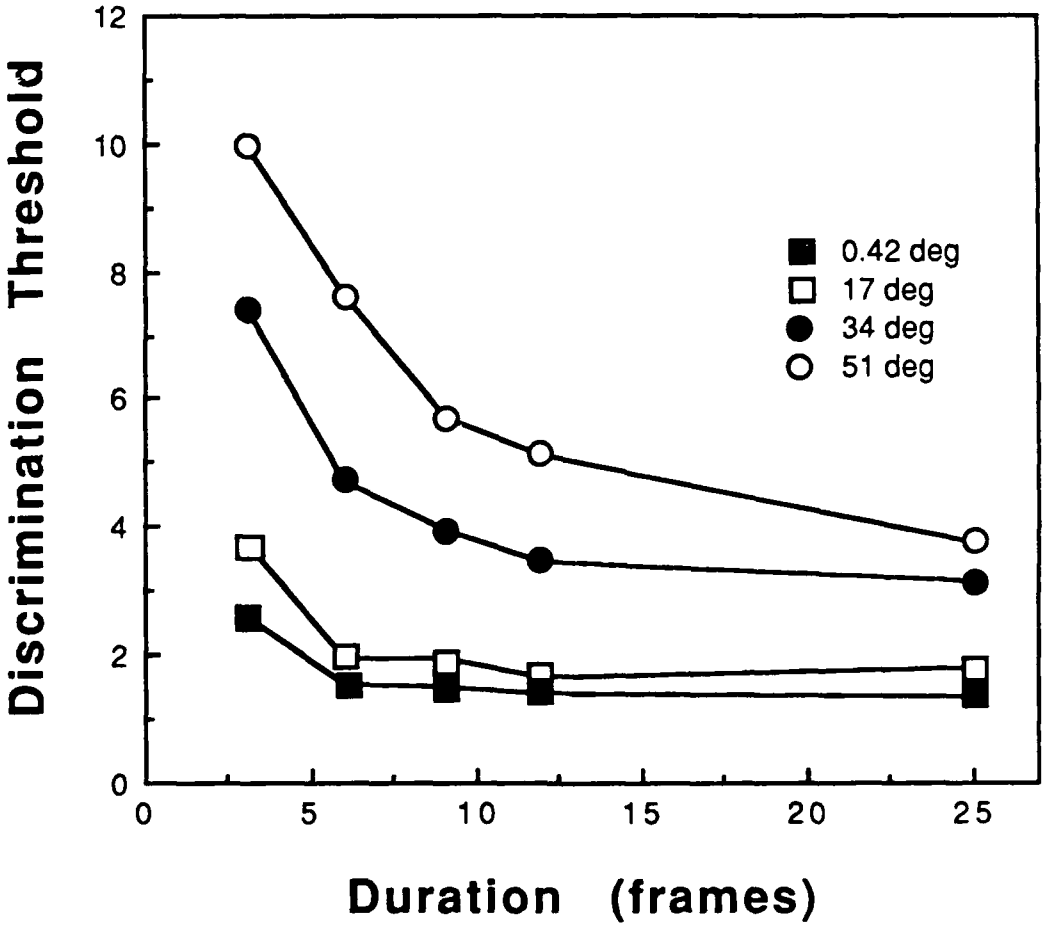
Discrimination Threshold
12
10
8
6
4
2
0
0
5
10
15
20
25
Duration (frames)
0.42 deg
17 deg
34 deg
51 deg

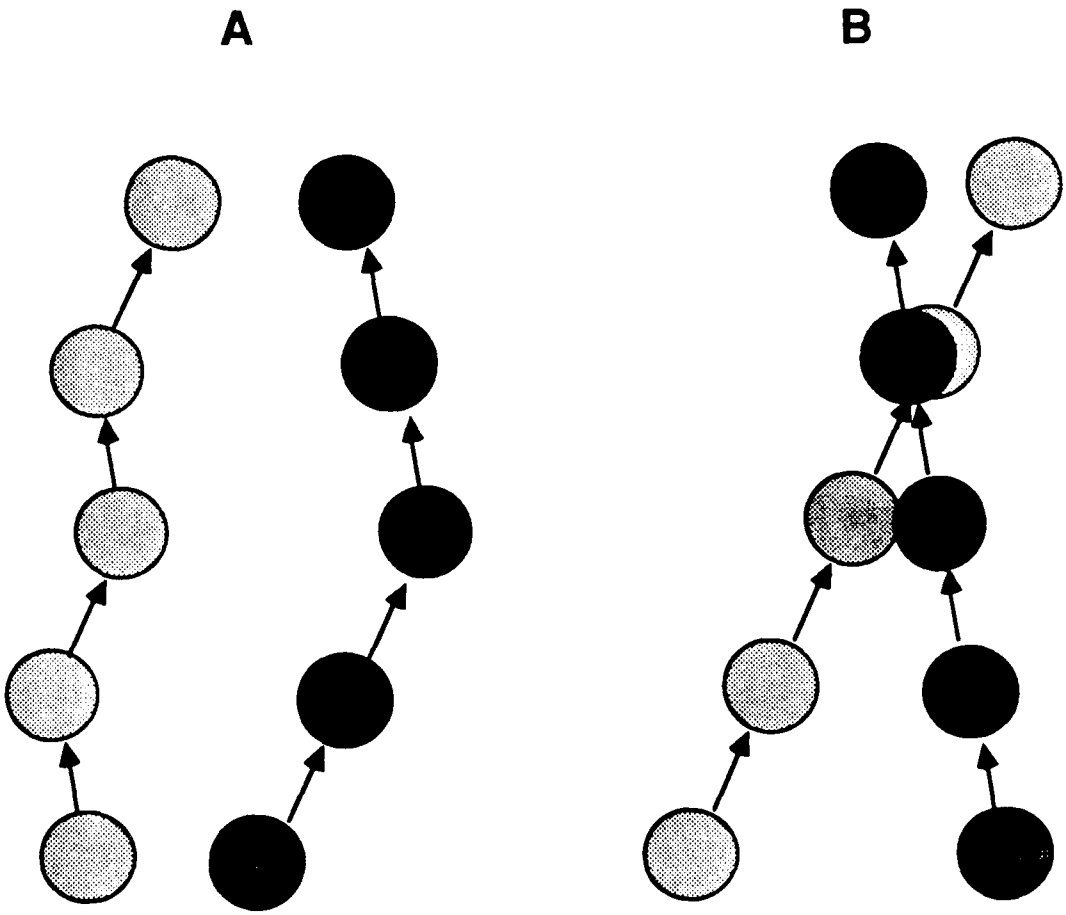
A
B
Random-Path
Fixed-Path

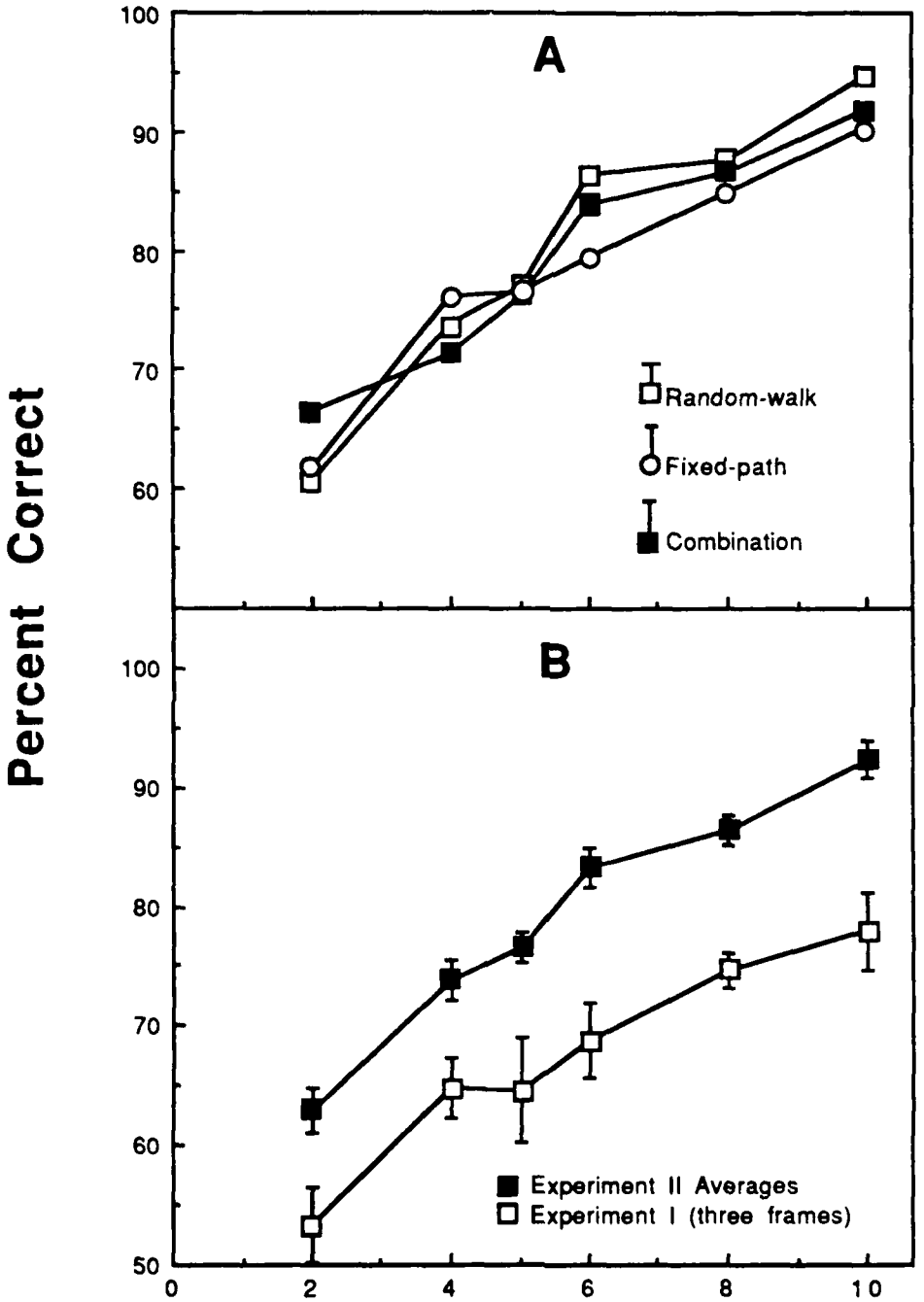
A
B
100
90
80
70
60
50
0
2
4
6
8
10
Random-walk
Fixed-path
Combination
Experiment II Averages
Experiment I (three frames)
Percent Correct
Separation Between
Distribution Mean Directions (deg)

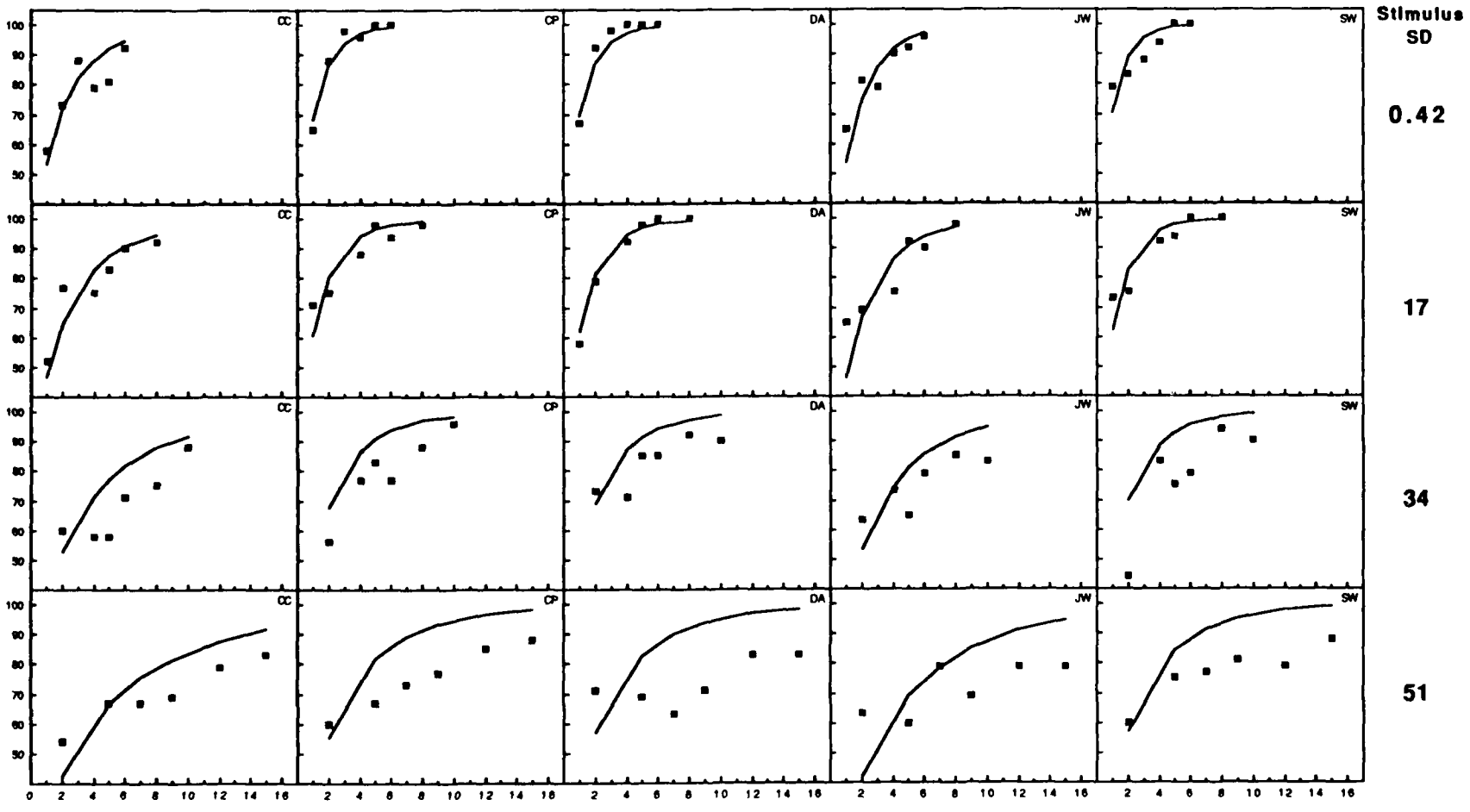
Percent Correct
Stimulus SD
0.42
17
34
51
CC
CP
DA
JW
SW
Separation Between Distribution Mean Directions (deg)

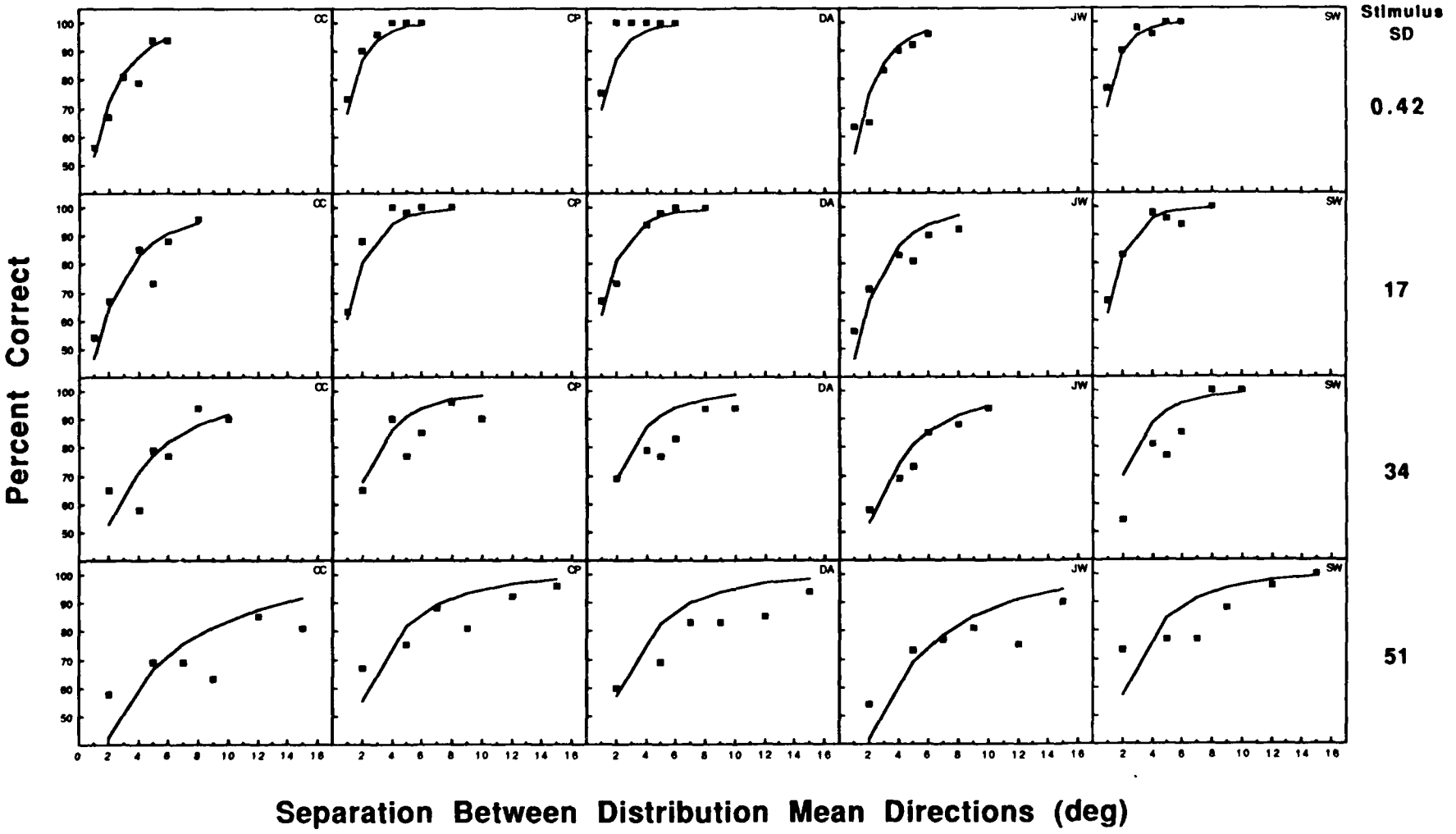
Percent Correct
CC
CP
DA
JW
SW
Stimulus SD
0.42
17
34
51
Separation Between Distribution Mean Directions (deg)

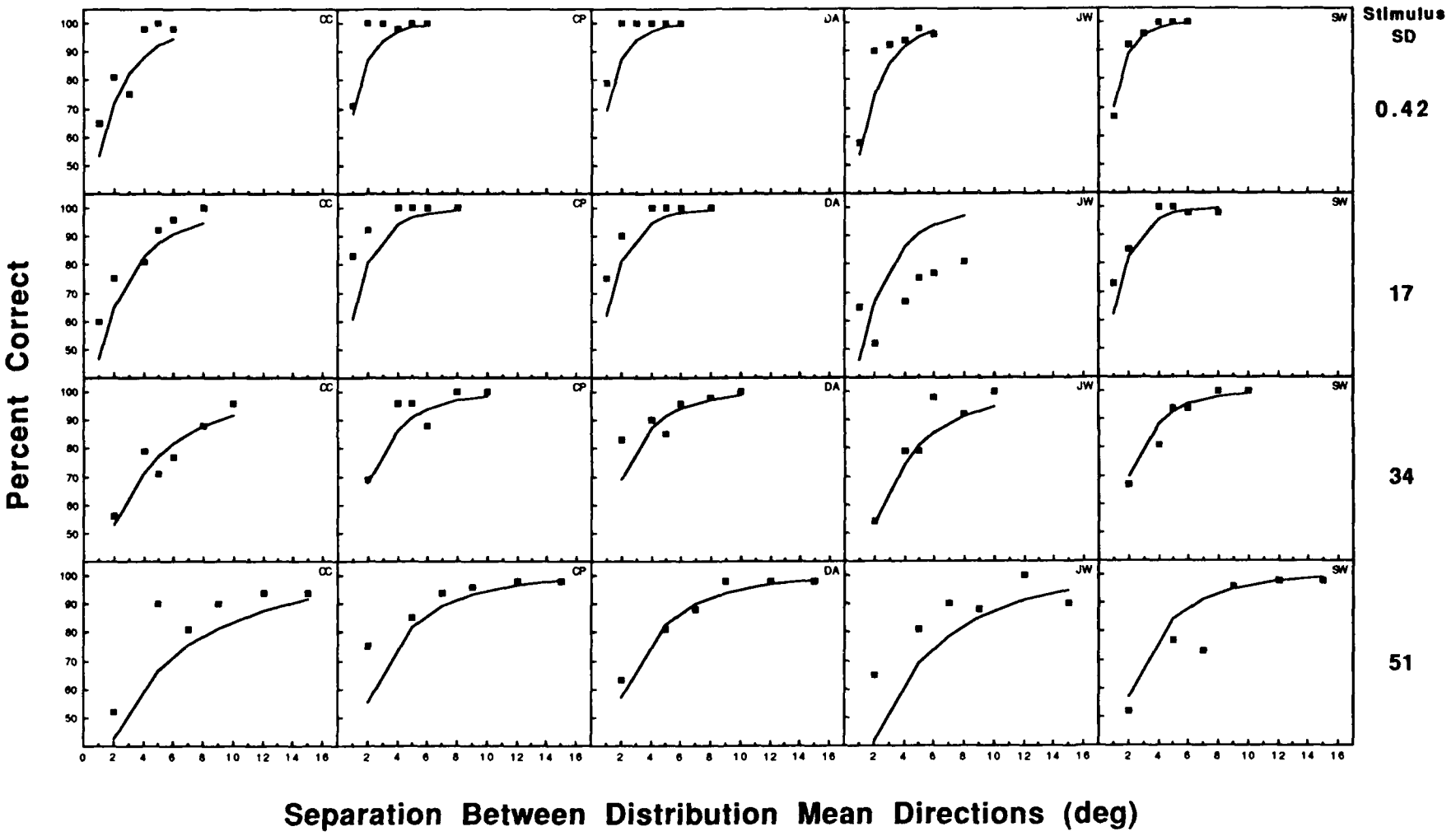
Percent Correct
CC
CP
DA
JW
SW
Stimulus SD
0.42
17
34
51
Separation Between Distribution Mean Directions (deg)

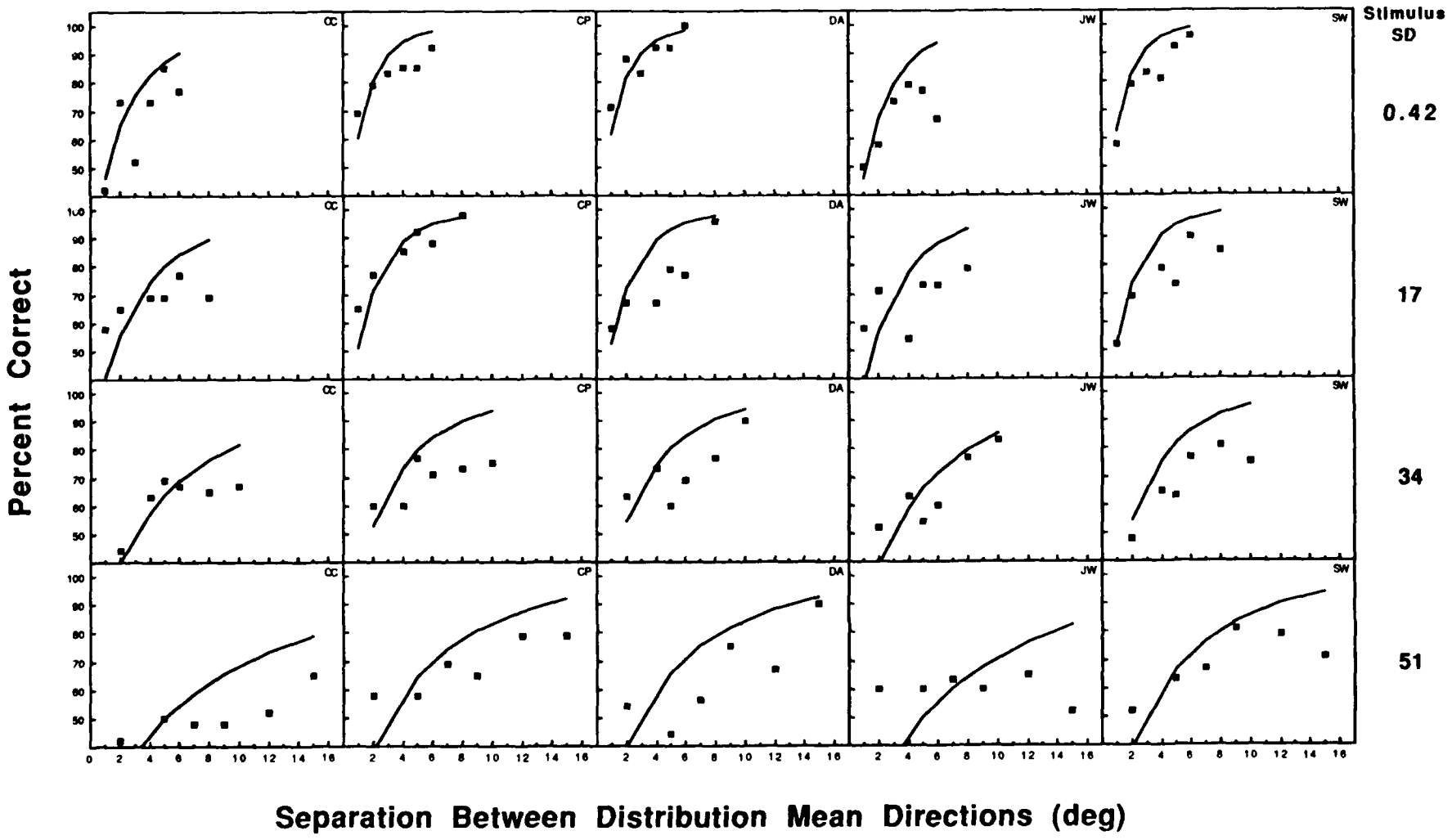
Percent Correct
CC
CP
DA
JW
SW
Stimulus SD
0.42
17
34
51
Separation Between Distribution Mean Directions (deg)

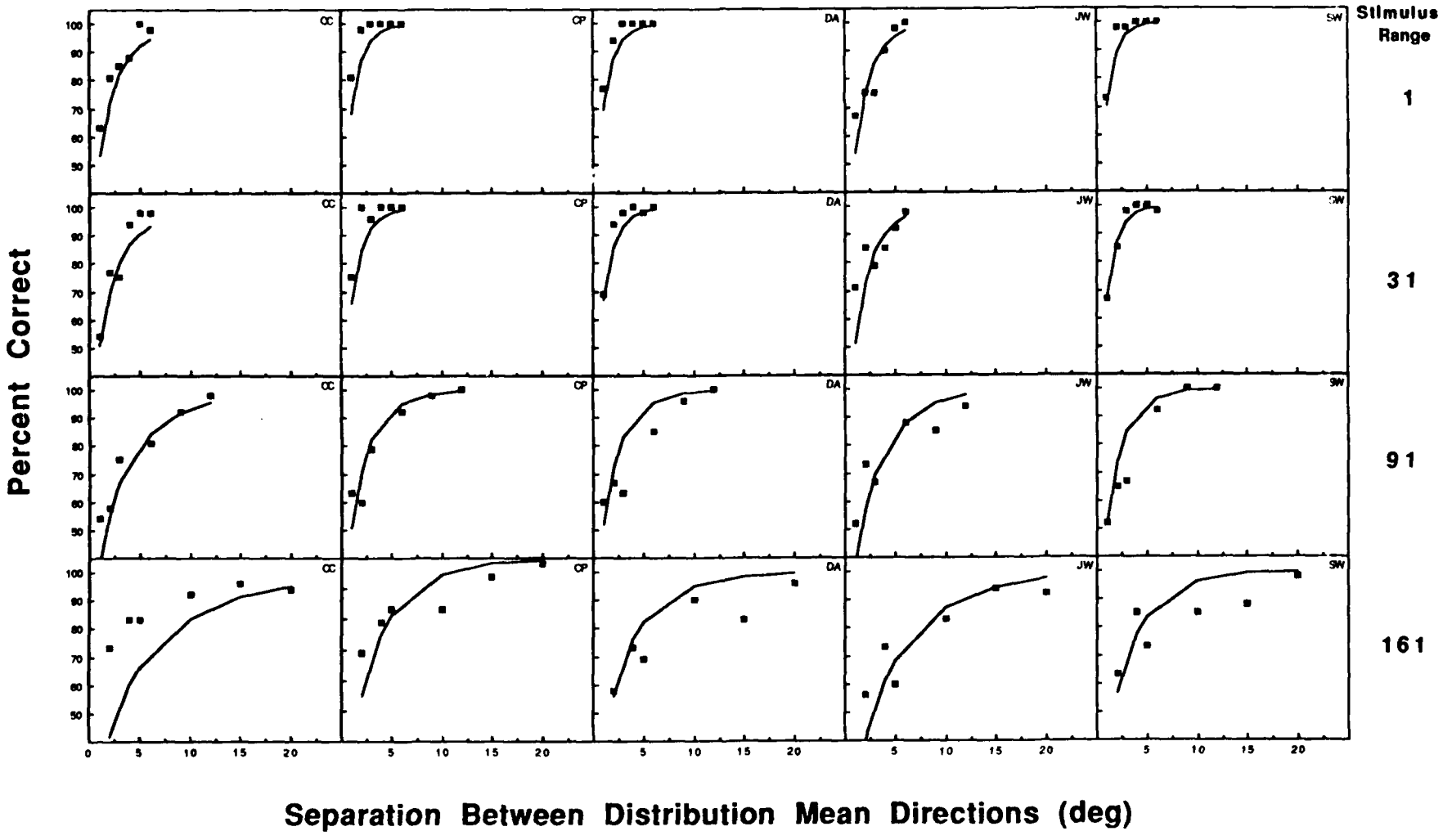
Percent Correct
CC
CP
DA
JW
SW
Stimulus Range
1
31
91
161
Separation Between Distribution Mean Directions (deg)

Project Two:

Reaction Times to Change in Speed and Direction of Motion

Robert Sekuler, Ehtibar Dzhafarov,
Juri Allik and Douglas W. Williams

INTRODUCTION

Dzhafarov and Allik proposed the Local Dispersion Model (LD-model) as a framework for interpreting detectability of planar rigid motion with an arbitrary time-position function (Dzhafarov et al., 1981; Dzhafarov, 1982; Dzhafarov et al., 1983; Dzhafarov and Allik, 1984). Predictions from the LD-model were consistent with data on kinematic thresholds and psychometric functions. Of particular importance for the present work, Allik and Dzhafarov (1984) found good quantitative agreement between their model and reaction times (RTs) to motion onset. Consistent with empirical findings (Ball and Sekuler, 1980; Tynan and Sekuler, 1982), the model predicted longer RTs to onset of slow motion than to fast motion.

In those studies of RT to motion onset, after some rest period the stimulus started to move with constant velocity . Now we have measured RTs in a more general situation: a target moves at a constant velocity for some random time, after which its velocity abruptly changes to another constant value. Observers must react as soon as the change in velocity is noticed. Our aim was to develop a theory that would account for the dependence of RT on the relationship between the two velocities. Figure 1 shows the various types of kinematic functions we used. The two phases of motion always had the same, horizontal, orientation; either they differed in speed (panels a and b), or they were in opposite directions (panel c). For each pair of velocities we analyzed mean RTs and standard deviations of RTs. Note, in Figure 1, that the first velocity of a pair sometimes took a zero value (panel a1); in such a case the *change of velocity* is identical to the *onset of uniform motion*, the condition

used by Tynan and Sekuler (1982).

[Insert Figure 1 about here]

Dzhafarov and Allik originally designed the LD-model to explain how the visual system distinguishes between a target's motion and non-motion. The model did not deal with detection of change in a particular parameter of motion, *e.g.* a change in direction or a change in speed. However, as we will show in this paper, a simple modification enables the LD-model to predict detectability of changes in velocity.

We will also show that one alternative model for RT to motion onset (Ball and Sekuler, 1980; Tynan and Sekuler, 1982; Allik & Dzhafarov, 1984) fails in the general case of velocity change. This alternative model asserts that reactions to motion onset are initiated when the target has moved through some constant, or critical, distance. The model is therefore referred to as a Constant Distance Model (CD-model).

In testing the models -- Local Dispersion and Constant Distance types -- we were primarily interested in quantitative predictions, and in the plausibility of their parameters' optimal values. Since there is theoretical interest in the way vision encodes direction and speed (for review: Sekuler, 1975; Nakayama, 1985), we also wanted to know whether a single framework could handle RTs to direction reversals as well as RTs to unidirectional speed changes.

Before turning to the details of our empirical research and theoretical analysis, consider a general postulate common to all theoretical treatments of RTs. The postulate is that reaction times are comprised of two additive components. One component, the decision time (t_D) is a function of stimulus

parameters such as velocity; the other component is residual time (t_R), the minimum time an observer needs to execute the required response. So, all models considered here agree that

$$RT = t_D + t_R \qquad [1]$$

The various models differ only in their interpretations of the t_D component.

The rest of the paper is organized as follows. First, we briefly discuss the LD-model and the CD-model as formulated for motion detection and for RTs to motion onset. There are two reasons for this discussion. First, these models are prototypes that we are going to transfer to the domain of velocity change; second, the onset of uniform motion is a particular case of velocity change, namely when the first of the two velocities is zero. We shall see that this subset of data forms a strong basis for evaluating the models. After the discussion of the original models, we present some plausible modifications for the situation investigated in our experiments. All the models will be formulated in strictly psychophysical terms: the characteristics of motion on which the decision is based, and the decision rule itself. After the models have been presented, experimental results will be described, and confronted by the models. Finally, the Discussion section considers one biologically plausible system of mechanisms able to extract the required characteristics from the stimulus.

LD-MODEL, CD-MODEL, AND PROPOSITION OF IDENTITY

The Local Dispersion Model (LD-model) has been described in more detail elsewhere (Dzhafarov, 1982; Dzhafarov and Allik, 1984; Dzhafarov *et*

al., 1983). Consider a two-dimensional luminance profile, L(x,y), whose position changes over time according to some arbitrary kinematic function, $k(t)=\langle k_x(t),k_y(t)\rangle$. The LD-model identifies two separable factors that limit motion detectability. One factor is spatio-temporal luminance fusion (or smearing) along the trajectory of motion; the other factor is a particular characteristic of the kinematic function, its "local dispersion".

Luminance fusion can take place if the kinematic function, k(t), is a high-frequency oscillation, and/or if the moving profile, L(x,y), has a repetitive structure. In either case we have high-frequency luminance flicker at every point of the motion trajectory. Adjacent flickers can fuse in a non-independent fashion because of spatio-temporal luminance integration in the visual system and in the display device. Whether the complete fusion takes place depends on both the kinematic function and the moving profile. If fusion is only partial, or it does not occur at all (as with the leading edge of a unidirectionally moving contour), then detectability of motion depends on the kinematic function only.

The model asserts that the detectability value is given by a moving average over the moving variance of the kinematic function, a value termed Local Dispersion (LD):

$$LD(t) = 1/(2T\tau^2) \int_{t-T}^{t} \int_{t_0-\tau}^{t_0} \int_{t_0-\tau}^{t_0} E[k(t_1),k(t_2)]^2 dt_2 dt_1 dt_0 \qquad [2]$$

where E is the Euclidean distance, τ is the time span of the moving variance (over the stimulus' kinematic function), T is the time span of the moving average (over the moving variance). Note that the term "local" in the name of

the model has a temporal rather than a spatial meaning: the LD-value is defined at every moment of time.

Equation 2 means simply that motion detectability is proportional to an average dispersion, or scatter, of a target's temporally close spatial positions. The local dispersion reflects the variance of spatial positions measured within a travelling temporal window, $[t_0 - \tau, t_0]$, and assigned to every moment t_0. At any moment, t, the LD-value is the mean of the moving variance between times t and t-T. Thus if T is zero, motion detectability is proportional to the maximal value of moving variance; if T is infinitely large, detectability depends on the grand mean of all variance values. Zero and infinity form the poles between which the actual value of T lies. Empirically, the ratio T/τ has been found to be a constant, 2, for all the data known to be relevant, though τ does vary with the display conditions and from one observer to the next. The τ is close to 0.5 sec for foveal absolute motion (*i.e.* one without a stationary reference near the motion). Figure 2 illustrates one of the computational algorithms that are equivalent to equation [2]. It will be discussed in more detail in Discussion.

[Insert Figure 2 about here]

Equation [2] represents LD as a particular characteristic, or feature of the stimulus' kinematic function; as a result it has the same ontological status as speed, distance, or acceleration. However the definition of a stimulus parameter on which the subjects might base their choice between "motion" and "no motion", constitutes only the first part of a complete psychophysical model. In the second part one should specify the decision rule for the particular

experimental task. Thus, for experiments with kinematic thresholds, like minimum amplitudes of oscillatory motions, one should assume that the motion is detected when the LD-value exceeds some critical level, C^2, where C is a distance-dimensioned parameter (notice that the LD is measured in squared distance units, *e.g.* min^2).

In using the LD-model to predict RTs one needs an assumption that links values of LD to the actual initiation of a reaction. Here again the simplest assumption is that a decision to react is made as soon as LD exceeds some critical value. In applying the LD-model to reaction times elicited by onset of motion, Allik and Dzhafarov (1984) showed that decision time, t_D, can be found from the equation:

$$V^2 t_D^4 (1 - 3t_D/5\tau)/(12T\tau) = C^2 \qquad [3]$$

V is the motion velocity; T, τ, and C have the same meaning as above. The t_D in equation [3] can be shown to be a decreasing function of V.

For RT experiments the LD-model gave numeric values of T, τ, and C that were similar to the values needed to account for kinematic thresholds and psychometric functions. This similarity is important. It means that in a reaction time experiment an observer actually obeys the experimenter's instructions, initiating reaction as soon as motion is *detected*. Putting it in other words, the similarity of parameters across experimental situations implies that an observer in a reaction time experiment uses the same criterion that an observer would use when kinematic thresholds were being measured. This implication, which we call the *Proposition of Identity*, suggests that

reaction time experiments should be considered as a one class of motion detectability experiment. Although they deal with motions well above threshold they reveal the same processes as do other types of experiments on motion detectability.

Only one other model has been applied to data on RT to motion onset, the Constant Distance (CD) Model (Ball and Sekuler, 1980; Tynan and Sekuler, 1982). It states that reactions to motion onset are initiated when the target has moved through some critical distance. When the motion has a constant velocity, V, the decision time, t_D, can be found from the simple formula

$$t_D = \Delta / V \qquad [4]$$

where Δ denotes the critical distance.

It's hard to formulate the Proposition of Identity for the CD-model because the model itself fails with data on kinematic thresholds. Except for oscillatory motion in a middle-frequency range (1-7 Hz), amplitude thresholds are not constant, and even over this limited range the "constant" varies with type of oscillation (Dzhafarov *et al.*, 1981). Nevertheless, some authors insist that the constant displacement rule does hold for very brief unidirectional motions (Cohen and Bonnet, 1972; Johnson and Leibowitz, 1976; Bonnet, 1977, 1982). If this suggestion were even approximately true, then the greatest precision in estimating critical displacement would be reached in the briefest possible motion, namely, an *instantaneous shift of position*. Then the Proposition of Identity for the CD model would reduce to the assumption that the parameter Δ, in equation [4] for reaction time, is close to the threshold for position shift.

THREE MODELS FOR RT TO VELOCITY CHANGE

We have described how the LD-model and the CD-model can account for RTs to motion onset. When uniform motion follows a rest period the solution is given by equations [3] and [4], in combination with the assumption expressed by equation [1]. We will now consider how these formulations can be modified for the general case of change from one velocity, V_0, to another, V_1. Recall that V_0 is the velocity of the first phase of motion that lasts for some random period and then abruptly changes to the second phase, with velocity V_1. The two motion phases have the same orientation, but different absolute values (speed) or signs (direction). Formally speaking, we seek to express RT as a function of $\langle V_0, V_1 \rangle$. From the original models we know a part of this function, the dependence of RT on pairs of the type $\langle 0, V \rangle$.

One simple solution suggests itself: reduce the general problem to the particular case for which the solution is already known. Specifically, assume that detection of velocity change, $\langle V_0, V_1 \rangle$, is structurally equivalent to detection of onset in the derived motion, $\langle 0, V_1 - V_0 \rangle$. By *structurally equivalent* we mean identical except for the values of the models' free parameters. Applying this scheme to both CD-model and LD-model, we get generalizations of equations [3] and [4].

For the Constant Distance Model:

$$t_D = \Delta(V_0)/|V_1 - V_0| \qquad [5]$$

For the Local Dispersion model:

$$|V_1 - V_0|^2 t_D^4 (1 - 3t_D/5\tau)/(12T\tau) = C(V_0)^2 \qquad [6]$$

For both equations, decision time depends upon an *equivalent* velocity rather than upon a directly measurable one. Therefore, as a reminder, we'll label the resulting models with the term "equivalent." So equation [5] describes the *equivalent* Constant Distance Model (eCD-model); equation [6] describes the *equivalent* Local Dispersion Model (eLD-model). The sign of V_0 can be always taken as positive, whereas the sign of V_1 is positive when the two phases are unidirectional, and negative when they have opposite directions.

In both models, Δ and C are functions of V_0, whereas t_R, as usual, is an independent random variable. Although it is not logically necessary, we assume that the parameters T and τ in the LD-model are unmodified by V_0. Moreover we will assume that the values of T and τ are the same as in motion detection experiments. Note that the second assumption is derivable from the first assumption together with the Proposition of Identity.

There is an alternative, perhaps more natural, way to generalize the Local Dispersion Model to the case of velocity change. Provided the first phase of $\langle V_0, V_1 \rangle$ lasts long enough ($\approx T+\tau$, estimated as 1.5 sec), LD will stabilize at $LD_0 = V_0^2\tau/12$ (Allik & Dzhafarov, 1984). Then, as velocity changes from V_0 to V_1, the value of LD also will change. We can postulate that velocity change will be detected when the difference between the current LD-value and the initial level LD_0 reaches some critical value. The critical value would depend, in general, on the LD_0 or, equivalently, on V_0:

$$|LD(t_D) - LD_0| = C(V_0)^2 \qquad [7]$$

The difference $LD(t_D) - LD_0$ is given explicitly in the following formula:

$$LD(t_D) - LD_0 =$$
$$(V_1-V_0)t_D^3(V_0\tau/6 + (V_1-2V_0)t_D/12 - (V_1-V_0)t_D^2/(20\tau))/T\tau \qquad [8]$$

Here again, V_0 is taken to be positive, and V_1 is positive if it and V_0 are in the same direction, and negative otherwise. Unlike the alternative version of LD-model discussed earlier (the eLD-model), the local dispersion model in equation [8] can be applied directly to the stimulus' actual, untransformed kinematic function. The only modification in the model is in the decision rule, which is a generalized version of one originally proposed by Allik and Dzhafarov. Therefore we can refer to a *generalized* Local Dispersion, or gLD, model.

EXPERIMENTAL PROCEDURE

The display consisted of 200 spatially-random, bright dots presented under computer control on a large, dim x-y cathode ray tube screen. The dots were 6 min in diameter, and dot-background contrast was set at 4-5 times threshold. The background luminance was about 1.5 cd/m^2. At the start of each trial, the dots appeared and began moving inside a 16 deg diameter circular aperture (see Figure 1). The dots moved horizontally in fixed spatial phase along parallel paths. When a dot reached the edge of the display it wrapped around, reappearing sometime later at the opposite edge. The dots' velocity was controlled by the size of steps, or displacements, from one frame to the next, keeping frame rate constant at 100 Hz. A new set of spatially random dots was

generated on each trial.

The experiment consisted of 35 different conditions, each corresponding to one velocity pair, $\langle V_0, V_1 \rangle$. They were tested one at a time in blocks of 50 trials. Over the entire study, each condition was tested on three different occasions, giving in total 150 trials per pair of velocities. The duration of V_0, or stimulus foreperiod, varied according to a uniform random distribution ranging from 1 to 2 seconds. Trials were initiated by the observer.

In thirty conditions, movement during both phases was in a rightward direction. In all these conditions, the subject reacted to a change in *speed* only (Figure 1a,b). Velocity pairs were chosen as pairs from the set of 0 (stationary dots), 1, 2, 4, 8 and 16 deg/sec, with the constraint that the two velocities in a condition could not be the same.

In another five conditions, speeds during both phases were the same. In these conditions, rightward motion during the foreperiod changed abruptly to leftward motion, with no change in speed (Figure 1c). In all these conditions, the subject reacted to a change in *direction* only. Speeds were 1, 2, 4, 8 and 16 deg/sec.

In addition we carried out an auxiliary experiment in order to find out whether any of the obtained results could be specifically associated with our choice of the number of dots in the display, 200. This experiment consisted of 39 different conditions, each corresponding to one of 13 velocity pairs, $\langle V_0, V_1 \rangle$, and one of three dot densities: 50, 100, or 200 dots per screen. A subset of the velocity pairs used in the main experiment was used here: ⟨0,1⟩, ⟨0,4⟩, ⟨0,16⟩; ⟨1,8⟩; ⟨2,1⟩; ⟨4,0⟩, ⟨4,16⟩, ⟨4,-4⟩; ⟨8,4⟩; ⟨16,0⟩, ⟨16,1⟩, ⟨16,2⟩, ⟨16,-16⟩, where the minus sign indicates leftward motion. In all other respects the auxiliary experiment was identical to the main one.

During analysis of the data, all responses less than 100 ms or greater than 1000 ms were discarded, as premature or indicative of the observer's momentary distraction. The number of discarded trials was fairly constant for all conditions, and constituted less than 5% of trials. Remaining trials were used to calculate arithmetic means and standard deviations of RTs for each condition.

One of the observers in the main experiment was an author of this report (RWS); the other observer (JF) was naive with respect to the purposes of the study. A third observer (JLM), also naive, served in the auxiliary experiment.

RESULTS

Figures 3 and 5 show the mean RTs for subjects JF and RWS, respectively. Figures 4 and 6 show corresponding standard deviations of RTs. All panels in every figure contain full set of data, for all $\langle V_1, V_0 \rangle$ pairs, but in each panel the data corresponding to one value of V_0 are "highlighted" (shown by squares) The data are plotted against two abscissae. The lower abscissa represents a measure of similarity between V_0 and V_1, namely $1/|V_1-V_0|^{0.5}$, arrayed linearly. Corresponding values of the difference $|V_1-V_0|$ are shown in the upper abscissa. The square-root operation in our similarity measure has been chosen to linearize the theoretical curves produced by one of the models, as discussed below.

[Insert Figure 3 about here]

[Insert Figure 4 about here]

[Insert Figure 5 about here]

[Insert Figure 6 about here]

One can notice the following main characteristics of the data.

(1) For a fixed V_0, means and standard deviations of the RTs both decrease as the difference between V_1 and V_0 increases.

(2) For a fixed value of $|V_1-V_0|$, RT means and standard deviations increase as the fore-speed, V_0, increases from 4 to 16 deg/sec. With slower forespeeds (between 0 and 4 deg/s) no such trend is discernible.

(3) In ordering both means and standard deviations of RTs, only absolute value of velocity difference, $|V_1-V_0|$, matters, irrespective of whether it represents velocity increment, velocity decrement, or direction reversal. Thus, means and standard deviations of RTs for the velocity pairs <4,0> and <4,8> are about the same, and fall between the corresponding RT moments for <4,16> and <4,1> (difference in velocities for the first two pairs is 4, for the second 12, and for the third 3 deg/s). In the direction reversal condition $|V_1-V_0|$ is equal to $2V_0$. For example, the difference in velocities for the pair <16,-16> is equal to 32 deg/s. Therefore, in compliance with the general pattern, the first two moments of the corresponding RT should be less than those for the pair <16,0>.

[Insert Figure 7 about here]

The scattergram in Figure 7 presents the results of the auxiliary experiment in which we varied the number of dots in the display (only mean RTs were analyzed for this experiment). The abscissa represents the mean RTs found with 200 dots in the display for various pairs of $\langle V_0, V_1 \rangle$. Against each mean RT obtained with 200 dots we have plotted the mean RT from the same $\langle V_0, V_1 \rangle$

condition obtained with 50 dots (crosses) and 100 dots (squares). The diagonal line represents the expected loci of data points if mean RT did not differ at all with number of dots in the display. The Friedman rank sums test shows that the difference between the 200 and 100 dot displays, on one hand, and the 50 dot display, on the other is significant ($0.025<p<0.05$). However, it is obvious from the figure that the fourfold change in dot density has a remarkably small effect on mean RT. Therefore our principle results are probably not restricted to the particular number of moving dots used in the main experiment.

Notice that characteristics (1) - (3) of the data are not sufficient to derive ordinal-scale predictions about velocity pairs with different values of both V_0 and $|V_1-V_0|$. A quantitative, model-bound analysis is needed for this purpose; such an analysis follows.

ANALYSIS

COMPUTATIONAL FORMULAS FOR E[RT] AND S[RT]. Formulas [5]-[8] (in combination with formula [1]) do not by themselves allow one to compute RT means and standard deviations. The formulas contain random variables with unknown distributions, t_R and $\Delta(V_0)$s (in the eCD-model) or $C(V_0)$s (in both versions of LD-model). For every combination of these parameters' values one can compute, using the formulas, a single value of RT. What we need instead is a theoretical prediction of RTs' first two moments, expected value, E[RT], and standard deviation, S[RT], for each pair $\langle V_0,V_1\rangle$. Since all models treat RT as a sum of decision time, t_D, and residual time, t_R, the task is reduced to finding the first two moments for the summands, $E[t_R]$, $S[t_R]$, and $S[t_D]$s and $E[t_D]$s, for each pair of velocities, $\langle V_0,V_1\rangle$.

$$E[RT(V_0,V_1)] = E[t_D(V_0,V_1)] + E[t_R]$$

$$S[RT(V_0,V_1)] = \{ S[t_D(V_0,V_1)]^2 + S[t_R]^2 \}^{1/2} \qquad [9]$$

The derivation of expressions for $E[t_D]$ and $S[t_D]$ in the eCD-model is straightforward. However, it's harder to derive exact computational formulas for t_D in the eLD- and gLD-models. These derivations require explicit assumptions about the distribution of parameter C. Because this would add extra free parameters, we wanted to avoid making such assumptions. Instead, we used approximate rather than exact formulas for the eLD- and gLD-model.

The required computational formulas for all the models are given in the Appendix. To account for mean RTs one has to adjust: (1) the value of $E[t_R]$; and (2) a measure of central tendency of distance-dimensioned parameters (Δ or C) corresponding to each value of V_0. To account for standard deviation of RTs one has to adjust: (1) the value of $S[t_R]$; and (2) a measure of variability of distance-dimensioned parameters (Δ or C) for each value of V_0. As we see, the number and the interpretation of the free parameters are identical in the three models. However the measures of central tendency and variability in these models are different. They are shown in Table A1 of the Appendix.

FITTING THE MODELS. There seems to be no conventional statistical procedure to estimate goodness of fit for both means and standard deviations, unless one makes explicit assumptions concerning the distributions of RTs. As explained before, we wanted to avoid assumptions that would add free parameters. Our aim was to determine whether one of the three models provided an account of the data that was substantially better than offered by the other models. This

The values are given in percentage terms in accordance with formula [10]. Thus, 2.52% means that, on average, the deviation of E[RT] predicted by the eLD-model from the empirical means makes 2.52% of the empirical values. For both means and standard deviations, the models can be ordered according to goodness-of-fit, eCD>eLD>gLD. However the differences are so small that no model can be rejected. For the means, each model yields values of MSRD less than 5%, obviously a very good fit. If 5% is acceptable for means, then the MSRD values provided by the models for standard deviations are comparably good.*

The small differences in values of fit make one wonder whether the obtained ordering of the models --eCD>eLD>gLD-- is replicable. In other words, can one expect to get the same ordering if the experiment is repeated? The results of the auxiliary experiment, with three different dot densities, suggest that the answer should be negative. The number of velocity pairs used in this experiment was rather small, and only one value of V_1 was paired with V_0 equal to 1, 2, and 8 deg/s. However the remaining three values of V_0, 0, 4, and 16 deg/s, were paired with more than one value of V_1 each, and these pairs can be used for model fitting. The results are presented in the bottom of Table 1.

* This can be shown as follows. The experiment was carried out in three blocks each containing about 50 trials per $\langle V_0, V_1 \rangle$ pair. The MSRD of the three sets of within-block means from the set of grand means is 4.19% for RS and 3.37% for JF, both values below 5%. One can conclude that the three blocks of measurements per condition are mutually consistent, and that their consistency is comparable with the MSRDs for E[RT] versus mean. Then it is natural to compare the MSRDs for S[RT] versus st. dev. with the level of consistency of the within-block st. dev.s. The latter is calculated as MSRD of the three sets of within-block st. dev.s from the set of grand st. dev.s. The level of consistency is 30.11% for RS and 56.76% for JF, which is well above the MSRDs provided by the three models. This informal consideration makes it obvious that the variability of st. dev.s is of a greater order of magnitude than the variability of means. If 5% is acceptance level for means, then 25% for standard deviations seems to be a very conservative estimate.

encouraged us to use a statistic whose theoretical distribution was not known. This statistic is the relative deviation, |predicted-observed|/observed, which expresses differences between predicted and observed values as a percentage of the observed value. This dimensionless measure can be used for both means and standard deviations, and seems to be a natural choice for inherently positive data, such as RTs. For the central tendency of relative deviations we used Mean Squared Relative Deviation, MSRD:

$$MSRD = \{\Sigma[\,(predicted - observed)/observed\,]^2/n\}^{1/2} * 100\% \qquad [10]$$

where summation is over all data points, that is for all n pairs, $\langle V_0, V_1 \rangle$. "Predicted" and "observed" should be replaced with either E[RT] and mean, or S[RT] and empirical standard deviation.

Theoretical predictions of the eLD-model are shown in Figures 3-6 by solid lines. The chosen format of the x-axis makes the predictions linear for mean RTs, and, in the range of velocity differences used, almost linear for standard deviations. The values of free parameters at which the minimum MSRD is achieved are given for all three models in the legends to Figures 3-6. In order not to impair readability we did not present the theoretical predictions of the two other models in the same plots, and presenting them separately would have taken too much space. The reason for singling out the eLD-model will be explained below. However it is not based on the values of minimum MSRD achieved by each model, as one can see from Table 1.

[Insert Table 1 about here]

When RTs were averaged over the three dot densities the ordering of the models was eLD>eCD>gLD. If the RTs corresponding to different numbers of dots were fitted separately, so that Δ and C are functions of both V_0 and dot density, then the resulting ordering was eLD>gLD>eCD. As we see, there is no consistent pattern in ordering of the models according to goodness-of-fit. In addition, the small differences between the MSRD values are at least in part due to the technical fact that we use precise computational formulas for the eCD-model, but only approximate formulas for the variants of the LD-model.

DIRECTION CHANGES VS. SPEED CHANGES. Figures 3-6 corroborate the ordinal characteristic of the data that we mentioned earlier: there were no qualitative differences between responses to 180^0 reversal of direction, on one hand, and responses to change in speed only, on the other. First, we verified that the fitted values of parameters were determined mainly by the unidirectional velocity pairs, rather than by the pairs with direction reversal; ignoring data involving a change in direction, and fitting models only to speed change data, produces very little change in the optimal values of models' parameters. This is not surprising since there were six times as many unidirectional velocity pairs as those with direction reversal. If RTs to direction reversals formed a qualitatively separate group they would deviate from predicted values more than do the RTs to speed change. This obviously is not the case.

The homogeneity of data, particularly the homogeneity of data for both speed changes and direction reversals, bears on the the general problem of velocity encoding in the visual system. However the data's homogeneity has an additional meaning within the framework of the LD-models. Unlike the case of unidirectional speed changes, direction reversals cause any dot to pass twice

over each spatial position along its trajectory. For spatial positions near the turn point this retracing leads to some luminance blur that could limit the applicability of the formulas based on kinematic function only (see the description of the LD-model above). The homogeneity of the data shows that the amount of blur in direction reversals was negligibly small.

BEST-FITTING PARAMETER VALUES. Since none of the models could be dismissed on the grounds of poor fit, we gave extra attention to the plausibility of the optimal values of the models' parameters.

The estimates of the time-dimensioned parameters, $E[t_R]$ and $S[t_R]$, are given in the legends to Figures 3-6. For the eLD-model these values are shown as the intercept points of the vertical axes with the theoretical curves (corresponding to infinitely large velocity difference, or zero closeness). The estimates of t_R given by the eCD-model, 214.5 ± 25.5 ms (RWS) and 209 ± 26.5 ms (JF), seem somewhat too high for residual times.** They are considerably higher than values reported for simple RT to long large high-intensity light flashes (Teichner and Krebs, 1972).

Estimates for the displacement-dimensioned parameters, C and Δ, are also given in the legends to Figures 3-6. Note that different measures of central tendency and variability were used for different models (see Table A1 in Appendix 1). For both means and standard deviation the greater the value of the displacement-dimensioned parameters, the greater the predicted rate of data decrease as the velocity difference increases.

Of primary interest for us here are the values corresponding to $V_0=0$, the particular case when the change of velocity is the onset of a uniform motion. If

** Here, for compactness of presentation, we use the format $E[t_R]\pm S[t_R]$. This should not be confused with anything like "confidence intervals" for $E[t_R]$. The $E[t_R]$ and $S[t_R]$ are independent estimates of two different parameters of a hypothetical distribution.

and only if the Proposition of Identity holds, RTs to motion onset can be considered as a particular paradigm of motion detection. Therefore by analyzing the values of C(0) and $\Delta(0)$ one can find out whether a particular model is consistent with the Proposition of Identity, *i.e.* whether these values are close to estimates of C and Δ derived from experiments on foveal absolute motion detectability. Recollect that $[C(0)]^2$ in the LD-model is the critical value of the local dispersion (formula 2) at which a target is judged as moving. The parameter $\Delta(0)$ in the CD-model (formula 4) is the critical distance that has to be traversed by a target to be judged as moving. In discussing detectability, the argument (0) in C(0) and $\Delta(0)$ is redundant and can be dropped.

In order to compare the values of C and Δ directly, one can bring them to a "common denominator" by expressing them in values of amplitude thresholds for a fixed kinematic function. The simplest choice of the kinematic function is the instantaneous shift of position. As it was stated in the introduction, if the CD-model can be related to detectability at all, then the amplitude threshold for instantaneous shift of position gives the most precise estimate of the critical displacement. In other words, the *equivalent threshold amplitude of instantaneous shift* for Δ (if the CD-model holds) is Δ itself. It can be shown that the *equivalent threshold amplitude of instantaneous shift* for C (if the LD-model holds) is equal to $C(6T/\tau)^{1/2} = 3.464C$ (since $T/\tau = 2$).

For their own data and from their reanalysis of others' data, Dzhafarov and Allik obtained values of C that fell between 0.1 - 0.7 min of arc. This can be considered a realistic confidence interval for E[C]. However in the analysis underlying these estimates -- for kinematic thresholds, psychometric functions, or reaction times -- C has been treated as a deterministic constant. The proposition that the estimated deterministic C-values are close to E[C] is,

strictly speaking, only a hypothesis. Therefore, in order to be absolutely sure, we will set more conservative interval 0.07 - 1.0 min of arc. It is hardly conceivable that E[C] for foveal absolute motion detection ought to fall outside these very generous boundaries. Indeed, the threshold amplitudes of instantaneous shift equivalent to these values are 0.25 - 3.5 min of arc, and the reported values of absolute shift thresholds lie well within these boundaries (Legge & Campbell, 1981). Obviously, these boundaries, 0.25 - 3.5 min of arc, should be considered also as a conservative interval for possible values of Δ.

Now, if the estimates of Δ and C are obtained from the reaction time rather than threshold experiments, then the Proposition of Identity can be judged to hold only if a central tendency of C and Δ falls between the established boundaries. *This is what we are going to check for the values of* C(0) *and* Δ(0) estimated from our present experiment.

The conservatism of our estimated boundaries for C and Δ makes the precise choice of the measure of central tendency for them rather unimportant: shift amplitudes of 0.24 min and 3.5 min certainly correspond to detection probabilities close to 0 and 1, respectively. However for direct comparison one should use a same measure of central tendency for both C and Δ. The measures estimated in our present analysis differ: it is $E[\Delta(0)]$ in the eCD-model, but it is $E[C(0)^{1/2}]^2$ in both versions of gLD-model. Fortunately we can easily avoid comparing moments of different types, since together with $E[C(0)^{1/2}]^2$ we get an independent estimation of $S[C(0)^{1/2}]^2$, and the sum of the two values should equal E[C(0)].

[Insert Figure 8 about here]

In Figure 8 the value of $E[\Delta(0)]$ is plotted along with the estimations of $E[C(0)]$ derived from the eLD-model and gLD-model, multiplied by 3.464 to represent the equivalent shift thresholds. The figure illustrates the fact that $E[\Delta(0)]$ estimated in the eCD-model grossly exceeds the very conservative upper limit we have set: estimates are 6.62 min (RWS) and 5.11 min (JF). In contrast, derived from the eLD-model, 1.92 min (RWS) and 1.13 (JF) not only fall between the conservative margins, but are also well within the more "realistic" interval 0.35 - 2.4 min of arc. The obvious conclusion is that tne considered variant of the LD-model generalization is nicely consistent with the Proposition of Identity, whereas the generalization of the CD-model is grossly inconsistent with it. In other words, if one accepts the eCD-model one must also accept the idea that the decision to react to the onset of motion is always made considerably after motion is actually detected.

The interpretation of the gLD-model is somewhat less certain. Although the two estimates, 2.76 min (RWS) and 1.75 min (JF), are within our conservative boundaries, the former value exceeds the "realistic" (with most probability also rather conservative) upper margin we have set. In combination with the fact that the fit provided by the gLD-model is slightly worse than that of the eLD-model, this makes the latter more preferable.

One may wonder why estimates of C(0) given by the gLD-model and eLD-model differ when the two models are coincident at V_0=0, where the models converge onto the original form of LD-model. The reason is that the two models, gLD and eLD, are fitted to the entire set of data, and that the common parameter t_R makes the fit for different V_0-values interdependent.

DISCUSSION

COMPARISON OF THE MODELS. It was disappointing not to be able to choose among the three models on the basis of their fits to data. However there are other grounds for making a choice. For one thing, the CD-model is clearly not consistent with the Proposition of Identity, the assumption that observers use the same criterion in reaction time and detection experiments. Therefore accepting the eCD-model for RTs to velocity change (including motion onset/offset) would uncouple RT experiments from detection experiments. Such an uncoupling would pose some difficult questions: (1) why should different criteria control the observer's decision in the two types of experiments? (2) why would an observer in a reaction time experiment not respond as soon as the motion had been detected, particularly since the instructions clearly encourage such behavior?

None of these difficulties attends the LD-model. It provides a unified framework for both detectability and RT data, and justifies considering the latter as a special case of the former. Although, there is no logical necessity for the Proposition of Identity, in the absence of other factors Occam's razor compels a preference for a model in which a single principle gives rise to various forms of motion detection.

Comparison of the two versions of the LD-model favors the eLD-version over the gLD-version. For one thing, the eLD-model fits data slightly better (see Table 1). Second, it is in better agreement with the Proposition of Identity: the estimation of E[C] for RWS is slightly over the "realistic" upper boundary we had set. In addition, the eLD-model can be computationally simplified with a better precision. However, the superiority of the eLD-version should be taken

with a reservation: the imprecision of the computational formulas for the gLD-model could itself have been responsible for the latter's worse performance.

NETWORKS OF BILOCAL CORRELATORS. In the rest of the paper we will consider the problem of realizability of the LD by a system of biologically plausible mechanisms. First, we will discuss this problem for the original motion detection model, then for the modifications of the eLD type. The LD-model for motion detection has been formulated as a highly specialized algorithm: it is applicable only if the moving stimulus, a spatio-temporal distribution of luminance, is represented by a single kinematic function defined at every moment. The problem of how the kinematic function is extracted from the stimulus flow-field is closely related to the general issue of the detection of non-rigid motion. Both questions are beyond the scope of this paper. However it is easy to see that a natural step toward solution of these problems is to realize the LD algorithm by the mass activation of more primitive and more universal mechanisms. The response of such a system to a rigidly moving pattern should be equal to the value of LD, but the system should perform computations over any spatio-temporal luminance distribution, however deviant from rigid motion.

One such system is suggested by the computational algorithm shown in Figure 2, and by the form in which moving variance is represented in equation [2]. Variance of a set of numbers is the mean squared deviation of the numbers from their mean, but it is also the mean squared pair-wise distance between the numbers themselves. Thus, in Figure 2, the variance of spatial positions within the travelling τ-window is proportional to the sum of all squared pair-wise distances between the spatial positions within the window. This suggests

the idea that the variance could be provided by a pool of mechanisms each tuned to a particular temporal and spatial distance. The output of such a mechanism should be proportional to the squared spatial distance to which it is tuned.

It is not difficult to see in these mechanisms a variant of the widely accepted idea that *bilocal correlators* are the elementary units of visual motion encoding (Reichardt, 1961; Barlow and Levick, 1963; van Doorn and Koenderink, 1982a,b; van de Grind, Koenderink, van Doorn, 1983). A bilocal correlator (Figure 9) consists of two units that sense the luminance profiles falling within two identical receptive regions separated by a distance Δs. The responses to the two luminance profiles are transmitted with a relative delay Δt into a comparator that performs a matching operation equivalent to a point-to-point correlation. For simplicity we will assume that a bilocal correlator is completely specified by Δt and the locations, s_1 and s_2, of its receiving regions, as if all bilocal correlators had the same size and the same sensitivity profile. This simplification will not affect the generality of our analysis, since it will be confined to rigid motion only. Note that Δs is the absolute value of the 2-D vector s_2-s_1 (or, if we consider only one-dimensional motion, s_2-s_1 is a signed number).

At a moment t, the output of a bilocal correlator, $\langle \Delta t, s_1, s_2 \rangle$, is maximal if a same luminance profile occupied locations s_1 and s_2 at times $t-\Delta t$ and t. With a threshold device connected to the comparator (see Figure 9) the mechanism becomes a detector with a Boolean output (0 or 1): it "fires" at time t if and only if the patterns at $(t-\Delta t, s_1)$ and (t, s_2) match. In order to make the bilocal correlators compute a moving variance one has to make two additional assumptions. First, the output of a mechanism $\langle \Delta t, s_1, s_2 \rangle$ should be multiplied by $\Delta s^2 = |s_2-s_1|^2$ (Figure 10, upper panel). Second, this output should last for τ-

Δt (Figure 10, lower panel).

The first assumption, multiplication by Δs^2, can be thought of in many "technical" variants. Thus, it could mean a straightforward amplification of the Boolean output, or it could mean that the number of identical mechanisms $\langle \Delta t, s_1, s_2 \rangle$ with Boolean outputs is an integer approximation of Δs^2. It might even have no structural meaning at all: since the output of any bilocal correlator is on a "labeled line", it can be "taken with appropriate weight" on a subsequent processing stage. Whatever the technical aspect of the multiplication, its *functional* meaning is the following. In a network of bilocal mechanisms designed for detection of motion, the detection of larger displacements conveys more evidence for motion than the detection of smaller ones. Therefore responses of the bilocal correlators should be taken with weights monotonically related to their spatial span, Δs. Squaring is a particular choice of such a monotonic function.

The second assumption, above, means that the total duration of the mechanism's cycle of activity, starting with activation of its first sensing unit, is τ : the cycle is comprised of the transmission time, Δt, and the output time, $\tau - \Delta t$. It follows that the maximum value of Δt a bilocal mechanism can have is τ, with instantaneous output. Since a new cycle of activity of any mechanism is initiated at every moment of time, the assumption should be complemented by some rules of interaction of subsequent cycles. For simplicity we assume no-interaction: the images of subsequent luminance profiles are transmitted to the comparator independently, and the overlapping outputs summed.

The summary output of a pool of the described mechanisms at any moment t will be proportional to moving variance of the kinematic function, provided all triads $\langle \Delta t, s_1, s_2 \rangle$, $\Delta t < \tau$, are represented in the pool. Of course, in a real

network the representation can be only provided by a finite set of mechanisms with overlapping spatial and temporal tuning. Therefore the proportionality of the network's output to the moving variance of the kinematic function can only be approximate.

Moving variance is only first step in the computational algorithm shown in Figure 2. To obtain LD one has to "smooth" the moving variance function by the T-length moving average operator. The realization of this final stage in terms of bilocal mechanisms is straightforward. Outputs of all the mechanisms should be assumed to feed into a leaky integrator, or "stack" of temporal span T (Figure 10, upper panel). Recall that the operation of averaging provides an estimation of the magnitude of the moving variance function. Thus if T is zero then the magnitude of the function will be the maximal single value of the moving variance; if T is infinitely large then the magnitude is the grand mean of all variance values. The actual value of T lies between these two poles. The output of the T-length "stack" at every moment t is proportional to the LD-value given by formula [2]. Namely, it is equal to $LD(t)T\tau^2$, and in decision rules postulated for threshold setting and reaction initiation it should exceed the critical level $C^2T\tau^2$.

In our description of bilocal correlators we have not specified whether the receiving areas of a correlator are defined in retinal or stimulus-plane coordinates. Either can be true. One could even assume that motion is processed on two levels: a lower-level retina-bound network of bilocal correlators, and a higher-level network with a built-in compensation for eye movements. The question is which of these networks is associated with motion detection. In most motion detection paradigms eye movements are negligible, so neither possibility can be rejected. Therefore, in the context of this paper, we will

consider implications for velocity change detection associated with each of these possibilities: what additional assumptions should be made, or how the network of bilocal mechanisms can be modified, to realize the eLD-model for detection of velocity changes.

If motion detection is defined in retinal coordinates, then the simplest hypothesis seems to be following.*** Since no fixation point was provided in our experiments, and the duration of the first phase of motion was relatively long (between 1 and 2 s), the observers certainly reached the smooth-pursuit stage of eye movement during this phase. Therefore, as velocity changes from V_0 to V_1, the retinal velocity changes from 0 to $|V_1-V_0|$, precisely the equivalence postulated in the eLD-model. One has to make additional assumptions to explain the increase of the critical level C as V_0 increases from 4 to 16 deg/s. One could assume that tracking of faster motions is associated with a higher level of "noise", or "residual activity" in the network of bilocal mechanisms, which (applying a standard signal-to-noise analysis) should be compensated for by adoption of a higher criterion level. The higher level of residual activity when tracking faster motions could be attributed to any or all of the following factors: first, the initial activity in the network, before a catching-up-with-V_0 saccade, is higher for faster motions; second, tracking could be less smooth for faster motions; finally, the average time of uninterrupted tracking decreases as motion velocity increases. Indeed, if tracking starts in the center of our 16 deg aperture, then for 8 and 16 deg/s velocities the eye would have to return to the center and start over again 1-2 times and 2-4 times, respectively. No returns would be necessary for velocities of 0-4 deg/s, so any residual activity following the initial catching-up-with-V_0 saccade would have more time to diminish.

*** The authors are indebted to Joseph Malpeli for substantial contribution into this hypothesis.

If motion detection is defined in stimulus-plane rather than retinal coordinates, then some form of the "adaptation" process should replace the physical zeroing of forespeed in the previous hypothesis. The required process can be provided by a re-calibration of the weights, or amplification coefficients, attached to the Boolean outputs of the bilocal correlators. Namely, at the second phase of motion, V_1, the output of any bilocal mechanism $\langle \Delta t, s_1, s_2 \rangle$, instead of being multiplied by $\Delta s^2 = |s_2 - s_1|^2$, should be multiplied by $|(s_2 - s_1) - V_0 \Delta t|^2$. Let us consider in more detail the process by which adjustment of weights might be achieved. During the first phase of the two-phase motion $\langle V_0, V_1 \rangle$ in every subset of the bilocal mechanisms corresponding to a given Δt the activated mechanisms in the network will group around the elements $\langle \Delta t, s, s+V_0\Delta t \rangle$ (provided that the subset is activated at all, *i.e* if the motion has lasted for more than Δt). This excitation pattern becomes stabilized after a time close to τ, and the task is to detect the change in this pattern. This goal is achieved by the re-calibration of the system of weights attached to the mechanisms, so that after the period τ the network would not respond until the excitation pattern changes. The re-calibration is mathematically equivalent to subtracting the spatial span $V_0\Delta t$ of the excited mechanisms from spatial spans of all mechanisms with a given temporal span Δt. After that, as long as the first phase of motion lasts, the reorganized system will be silent: the responses of the excited mechanisms will be multiplied by $|(s+V_0\Delta t) - s - V_0\Delta t|^2 = 0$. As soon as the velocity changes to V_1, the now-reorganized system will respond like the original system would have responded to $V_1 - V_0$: the outputs of the excited mechanisms $\langle \Delta t, s, s+V_1\Delta t \rangle$ will be multiplied by $|(s+V_1\Delta t) - s - V_0\Delta t|^2 = |(V_1 - V_0)\Delta t|^2$. The hypothetical process of re-calibration, providing a transient character of

motion detection network activity, could be referred to as "self-inhibition".

To understand why the reorganization of weights also affects the critical level C, one could again assume that silencing of the network is only relative, and that a "residual activity" is higher for faster motions. One could even repeat one of the arguments suggested in the retina-bound-network hypothesis: that higher residual activity is due to the higher initial activity realizing detection of the first phase of motion. Also, the necessity to restart tracking after encountering aperture border could be associated with a re-activation of the network even if defined in stimulus coordinates. Alternatively, or in addition, one could assume that spatial tuning characteristics of bilocal mechanisms overlap, and that the degree of overlap increases with Δs. Consider the set of bilocal correlators with a given span Δt. Suppose that during the V_0-phase three groups of mechanisms were activated, with peak spatial tuning to $V_0\Delta t$, $V_0\Delta t+\varepsilon$, and $V_0\Delta t-\varepsilon$. The assumption we have made above means that ε is greater for greater $V_0\Delta t$, and thereby for greater V_0. One of the values, $V_0\Delta t$, $V_0\Delta t+\varepsilon$, or $V_0\Delta t-\varepsilon$ should be chosen to serve as an effective zero in the modified system of weights attached to the mechanisms with the temporal span Δt. At the present level of analysis it is immaterial whether the effective zero is chosen at random amidst the activated units, or whether there is a mechanism determining the "central" value $V_0\Delta t$ more precisely. Whatever the rule, it is clear that the "silencing" of the network at the end of the V_0-phase, after the weights have been re-calibrated, is only relative. For example, if $V_0\Delta t$ operated as an effective zero point, then the responses of the mechanisms tuned to spatial shifts $V_0\Delta t+\varepsilon$ and $V_0\Delta t-\varepsilon$ will each be taken with the weight $|(V_0\Delta t+\varepsilon)-V_0\Delta t|^2 = \varepsilon^2$. Applying a standard signal-to-noise analysis, greater values of ε will require the adoption of higher critical levels.

CONCLUSION. We conclude this paper with a brief recapitulation of the main results. First, a modified variant of the LD-model accounts for the RTs to velocity changes $\langle V_0, V_1 \rangle$. The essence of this modified variant is the application of the original LD-model to the detection of motion onset in $\langle 0, V_1 - V_0 \rangle$, with the critical level C being a (non-strictly) increasing function of V_0. Second, at $V_0=0$, where the modified and the original versions of the model logically coincide, the estimated value of C was found to be in a good agreement with the estimates obtained from other motion detectability experiments. Third, the changes in speed and direction are treated in the same way. In both cases, the perceptual response seems to depend upon the algebraic difference between V_1-V_0. Finally, both the original and the modified versions of the LD-model can be realized by mass activation of a network of bilocal mechanisms.

Some of the characteristics we have attributed to these bilocal mechanisms do not seem to have obvious analogues in known physiological structures. The long duration of the mechanisms' activity, about 0.5 s, suggests that the analogues should be sought in the neuronal *circuitry* rather than in single neurons. However physiological considerations do not seem to be most imminent problem at present. Many questions remain to be answered in a purely psychophysical plane. Thus, it is not clear how the described network can provide the concordant shift of τ and C as the detection changes from absolute to relative motion (Dzhafarov and Allik, 1984). Also, it remains to be found out, whether the network can account for the detection of non-rigid planar motion. This seems to be a very important line for future analysis, which

should show whether the model can indeed be considered as a good generalization of the original algorithm for local dispersion.

Speaking specifically about the problem of RTs to velocity changes, an important remaining problem is to experimentally test the hypothesis of eye movements against the hypothesis of re-calibration of weights. Another obvious continuation of the present work would be to use two dimensional velocity pairs, i.e. pair of V_0 and V_1 that differ only in the orientation of their motions. The eLD-model, described in this paper, can be applied without modification to this situation if $|V_1-V_0|$ is understood to be the length of a vectorial difference, rather than as the absolute value of a scalar.

Acknowledgments. This work was partially supported by a grant from the U.S. Air Force Office of Scientific Research, AFOSR 85-0370. The authors are grateful to Joseph Malpeli for the critical reading of the manuscript.

APPENDIX

COMPUTATIONAL FORMULAS FOR eCD-MODEL, eLD-MODEL, AND gLD-model

Formulas for $E[t_D]$ and $S[t_D]$ for the eCD-model can be derived from formula [5]:

$$\cdot[t_D(V_0,V_1)] = \cdot[\Delta(V_0)]/|V_1-V_0| \qquad (A1)$$

where the period denotes either of two moments, E and S. This formula together with the general equations [9] form the computational basis for the eCD-model-predictions.

The situation is more complicated with the two models that are based on LD-model. In formulas [6] and [8] there is no function of $C(V_0)$ on which t_D depends linearly. Strictly speaking, to deal with the problem we have to specify the exact form of the 8 distributions of $C(V_0)$s, V_0 = 0, 1, 2, 4, 8, and 16 deg/s. However such an analysis would add more free parameters and make the LD-model-based versions incomparable with the simple application of the eCD-model.

Fortunately there is a way to avoid such an awkward analysis. We can assume that the decision time, t_D, is considerably smaller than τ (0.5s). Then in formulas [6] and [8] all the summands except those containing the lowest power

of the fraction t_D/τ can be omitted. This assumption gives us approximate formulas in which t_D depends linearly on some (nonlinear) function of $C(V_0)$. Now the formulas for the moments can be easily derived. For the eLD-model we have:

$$.[t_D(V_0,V_1)] = .[C(V_0)^{1/2}](12T\tau)^{1/4}/(|V_1-V_0|)^{1/2} \qquad \text{(A2)}$$

For the gLD-model we have:

$$.[tD(V_0,V_1)] = .[C(0)^{1/2}](12T\tau)^{1/4}/|V1|^{1/2} \qquad \text{if } V_0 = 0$$

$$.[tD(V_0,V_1)] = .[C(V0)^{2/3}](6T)^{1/3}/(|V_1-V_0|)^{1/3} \qquad \text{if otherwise} \qquad \text{(A3)}$$

Here again the period stands either for E or S, and the predictions for E[RT] and S[RT] are derived by combining the formulas with the general equations [9]. The values of T and τ in application of the formulas were put equal to 1s and 0.5s, respectively. The value of T/τ has been shown to equal 2 for all detection experiments, whereas the value of τ varied in the region 0.4 - 0.7s. The value 0.5s for present analysis was chosen simply as a "round" number. We have checked that change of τ value in the region 0.4 - 0.7s leads to only minor changes in predicted values. All three models have the same two time-dimensioned parameters, $E[t_R]$ and $S[t_R]$. The following table summarizes the sets of the models' distance-dimensioned parameters.

[Insert Table A1 about here]

TABLE 1. MINIMUM MSRD VALUES

	mean RT			st. dev. of RT		
SUBJECT	**eCD**	**eLD**	**gLD**	**eCD**	**eLD**	**gLD**
RWS	3.57%	3.69%	4.80%	13.66%	13.67%	14.66%
JF	2.52%	2.67%	3.12%	18.92%	20.17%	20.88%
JLM*	2.63%	1.91%	2.66%			
JLM**	2.54%	2.12%	2.49%			

---

* auxiliary experiment, averaged over 3 dot densities

**auxiliary experiment, 3 dot densities fitted separately

TABLE A1. DISTANCE-DIMENSIONED PARAMETERS

MODEL	PARAMETER	CENTRAL TENDENCY	VARIABILITY
eCD-model	$\Delta(V_0)$	$E[\Delta(V_0)]$	$S[\Delta(V_0)]$
eLD-model	$C(V_0)$	$E[C(V_0)^{1/2}]^2$	$S[C(V_0)^{1/2}]^2$
gLD-model	$C(V_0)$	if $V_0=0$ $E[C(0)^{1/2}]^2$	$S[C(0)^{1/2}]^2$
		if $V_0\neq 0$ $E[C(V_0)^{2/3}]^{3/2}$	$S[C(V0)^{2/3}]^{3/2}$

REFERENCES

Allik J. and Dzhafarov E. N. (1984) Reaction time to motion onset: Local dispersion model analysis. Vision Research, **24**, 99-101.

Ball K. and Sekuler R. (1980) Models of stimulus uncertainty in motion perception. Psychological Review, **87**, 435-469.

Barlow H. B. and Levick W. R. (1963) The mechanisms of directionally sensitive units in rabbit's retina. Journal of Physiology (London), **178**, 377-504.

Bonnet C. (1977) Visual motion detection models: Features and frequency filters. Perception, **6**, 491-500.

Bonnet C. (1982) Thresholds of motion perception. In: A. H. Wertheim, W. A. Wagenaar and H. W. Leibowitz (Eds) Tutorials on Motion Perception. New York: Plenum, 41-79.

Cohen R. L. and Bonnet C. (1972) Movement detection thresholds and stimulus duration. Perception & Psychophysics, **12**, 269-272.

Dzhafarov E. N. (1982) General model for visual motion detection. Studia Psychologica, **24**, 193-198.

Dzhafarov E. N. and Allik J. (1984) A general theory of motion detection. In: M. Rauk (Ed) Computational Models in Hearing and Vision. Tallin: Estonian Academy of Sciences, 77-84.

Dzhafarov E. N., Allik J. and Linde N. D. (1983) Detection of oscillatory movement. Voprosy Psikhologii, **3**, 90-96 (in Russian).

Dzhafarov E. N., Allik J., Linde N. D. and Plastolov V. K. (1981) Comparative analysis of frequency-amplitude threshold functions for real and apparent motion. Psikhologicheskii Zhurnal, **2**, 73-78 (in Russian).

Johnson C. A. and Leibowitz H. W. (1976) Velocity-time reciprocity in the perception of motion: Foveal and peripheral determinations. Vision Research, **16**, 177-180.

Legge G. E. and Campbell F. W. (1981) Displacement detection in human vision. Vision Research, **21**, 205-213.

Nakayama K. (1985) Biological image motion processing: A review. Vision Research, **25**, 625-660.

Reichardt W. (1961) Autocorrelation, a principle for the evaluation of sensory information by the central nervous system. In: Rosenblith W. A. (Ed) Sensory Communications, Massachusetts: MIT Press, 303-317.

Teichner W. H. and Krebs M. J. (1972) Laws of the simple visual reaction time.

Psychological Review, **79**, 344-358

Tynan P.D. and Sekuler R. (1982) Motion processing in peripheral vision: Reaction time and perceived velocity. Vision Research, **22**, 61-68.

Van Doorn A. J., and Koenderink J. J. (1982a) Temporal properties of the visual detectability of moving spatial white noise. Experimental Brain Research, **45**, 179-188.

Van Doorn A. J., and Koenderink J. J. (1982b) Spatial properties of the visual detectability of moving spatial white noise. Experimental Brain Research, **45**, 189-195.

Van de Grind W. A., Koenderink J. J. and Doorn A. J. van (1983) Detection of coherent movement in peripherally viewed random-dot patterns. Journal of the Optical Society of America, **73**, 1674-1683.

FIGURE CAPTIONS

FIGURE 1. Display and types of kinematic functions used. Multiple-dot patterns like that shown in the upper left panel moved horizontally inside a 16 deg diameter circular aperture. The motion consisted of two phases, with constant velocities represented by the slopes of the straight lines in the panels a, a1, b, b1, and c. The two motions were either in the same direction (panels a, b), or in opposite directions (panel c). In the latter case the two phases had equal speeds. For unidirectional phases, the change in speed could be incremental (panel a) or decremental (panel b), including the cases of motion onset (panel a1) and offset (panel b1). See Procedure for details.

FIGURE 2. Schematic presentation of an algorithm equivalent to formula [2] of the LD-model. Right panel shows a complex kinematic function with temporal window of length τ travelling in time and computing the variance of spatial positions within it. Two positions of the τ-window are shown in the figure: $[t'-\tau,t']$ and $[t''-\tau,t'']$. The results of the computations form the moving variance function shown in the middle panel. Thus, the value of this function at moment t' is equal to the variance of spatial positions passed between the moments $t'-\tau$ and t'. The moving variance function is smoothed by travelling window of length T. This smoothing produces the LD-function

shown in the left panel. Two positions of the T-windows are shown in the figure: [t*-T,t*] and [t**-T,t**]. Thus the LD-value at the moment t* is equal to the mean value of the moving variance between t*-T and t*.

FIGURE 3. Mean RT versus "square-root-closeness" of V_1 to V_0, $|V_1 - V_0|^{-1/2}$. Subject JF. Every panel contains the mean RTs for all pairs $\langle V_0, V_1 \rangle$, but the means corresponding to one value of V_0 (given in insets) are "highlighted" (represented by squares), whereas the remaining values serve as a background (dots). Filled squares correspond to velocity increase ($V_1 > V_0$), empty squares with central dots correspond to velocity decrease ($V_1 < V_0$), crossed squares represent the direction reversal condition ($V_1 = -V_0$).

Solid lines are theoretical predictions of the eLD-model: $E[t_R]$ is equal to 180.5 ms (intercept with the vertical axis), central tendency of C (from panel 0 through 16) is equal to 0.28 - 0.31 - 0.37 -0.39 - 0.65 - 1.37 (min arc). These values correspond to the slopes of the solid lines.

Optimal parameters for the eCD-model: E[RT] = 209.0 ms; central tendency of Δ (from panel 0 through 16) is 5.11 - 5.13 - 6.30 - 7.99 - 13.66 - 28.21 (min arc).

Optimal parameters for the gLD-model: E[RT] = 163.0 ms; central tendency of C (from panel 0 through 16) is 0.45 - 1.08 -1.63 - 2.26 - 4.07 - 8.43 (min arc).

See Table A1 for the exact meaning of "central tendency".

FIGURE 4. Standard deviation of RT versus "square-root-closeness" of V_1 to V_0, $|V_1 - V_0|^{-1/2}$. Subject JF. Every panel contains the st. dev.s for all pairs $\langle V_0, V_1 \rangle$, but the st. dev.s corresponding to one value of V_0 (given in

insets) are "highlighted" (represented by squares), whereas the remaining values serve as a background (dots). Filled squares correspond to velocity increase ($V_1 > V_0$), empty squares with central dots correspond to velocity decrease ($V_1 < V_0$), crossed squares represent the direction reversal condition ($V_1 = -V_0$).

Solid lines are theoretical predictions of the eLD-model: $S[t_R]$ is equal to 22.0 ms (intercept with the vertical axis); variability of C (from panel 0 through 16) is equal to 0.046 - 0.067 - 0.084 - 0.058 - 0.118 - 0.237 (min arc). These values roughly correspond to the slopes of solid lines.

Optimal parameters for the eCD-model: S[RT] = 26.5 ms; variability of Δ (from panel 0 through 16) is 2.901 - 2.928 - 4.697 - 4.383 - 9.530 - 17.731 (min arc).

Optimal parameters for the gLD-model: S[RT] = 18.0 ms; variability of C (from panel 0 through 16) is 0.058 - 0.281 - 0.411 - 0.449 - 0.895 - 1.833 (min arc).

See Table A1 for the exact meaning of "variability".

FIGURE 5. Same as Figure 3, but for subject RWS.

Solid lines are theoretical predictions of the eLD-model: $E[t_R]$ is equal to 180.5 ms; central tendency of C (from panel 0 through 16) is equal to 0.49 - 0.49 - 0.39 - 0.50 - 0.88 - 1.64 (min arc).

Optimal parameters for the eCD-model: E[RT] = 214.5 ms; central tendency of Δ (from panel 0 through 16) is 6.62 - 7.12 - 6.19 - 8.24 - 15.43 - 28.13 (min arc).

Optimal parameters for the gLD-model: E[RT] = 162.0 ms; central tendency of C (from panel 0 through 16) is 0.72 - 1.4 - 1.7 - 2.66 -4.96 - 9.62 (min

arc).

FIGURE 6. Same as Figure 4, but for subject RWS.

Solid lines are theoretical predictions of the eLD-model: $S[t_R]$ is equal to 19.5 ms, variability of C (from panel 0 through 16) is equal to 0.065 - 0.058 - 0.053 - 0.096 - 0.169 - 0.189 (min arc).

Optimal parameters for the eCD-model: S[RT] = 26.5 ms; variability of Δ (from panel 0 through 16) is 3.024 - 2.930 - 3.278 - 5.378 - 11.219 - 14.660 (min arc).

Optimal parameters for the gLD-model: S[RT] = 18.0 ms; variability of C (from panel 0 through 16) is 0.077 - 0.245 - 0.309 - 0.616 - 1.106 - 1.542 (min arc).

FIGURE 7. Results of the auxiliary experiment. Mean RTs for patterns with 50 and 100 dots at each value of $\langle V_0, V_1 \rangle$ are plotted against mean RTs with patterns of 200 dots for the same $\langle V_0, V_1 \rangle$.

FIGURE 8. Equivalent amplitude of instantaneous displacement corresponding to theoretical estimations of distance-dimensioned parameters, C and Δ, at $V_0 = 0$. If the Proposition of Identity holds, the equivalent amplitude should be equal to the minimal detectable amplitude for instantaneous displacement. Clear area in the figure corresponds to the range of realistic values for the amplitude threshold. Sparsely stippled area corresponds to the values that are beyond the realistic limits but still within the conservative boundaries set in this paper. Densely stippled area corresponds to the range that certainly cannot include possible values of the threshold amplitude. See Analysis for details.

FIGURE 9. Basic structure of a bilocal correlator. Two identical receptor areas centered at s_1 and s_2 feed into a matching device, or comparator. Information transmission from the s_1-area to the comparator takes by Δt longer than transmission from the s_2-area. Therefore the images of luminance profiles falling on the two areas at two moments separated by Δt reach the comparator simultaneously. The images are supposed to be analogues of spatial maps of excitation, and the comparator performs an operation analogous to a point-to-point correlation. If the value of this correlation exceeds a critical level set by the subsequent threshold device, the mechanism generates a signal. See Discussion for details.

FIGURE 10. Basic structure of a bilocal correlator that implements the LD-algorithm of Figure 2. Upper panel: the output of correlators is amplified proportionally to the squared value of their spatial spans, and is fed into a leaky integrator. The integrator acts as a stack whose memory span is T: at every moment t it adds the summary input to its content and "forgets" the input received at the moment t-T. Lower panel: the bilocal correlator's signal that is initiated by a given pair of luminance profiles, separated in time by Δt, lasts for τ-Δt. So the total cycle of activity of any correlator takes a constant time, τ. See Discussion for details.

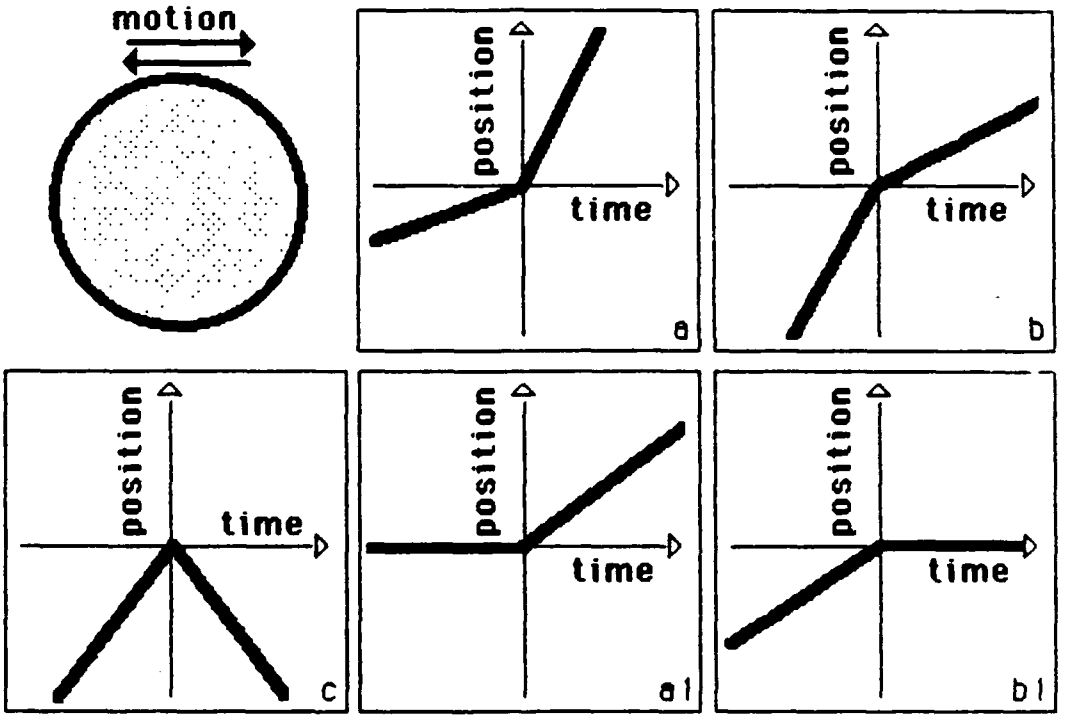
motion
position
time
a
position
time
b
position
time
c
position
time
a1
position
time
b1

FIGURE 1

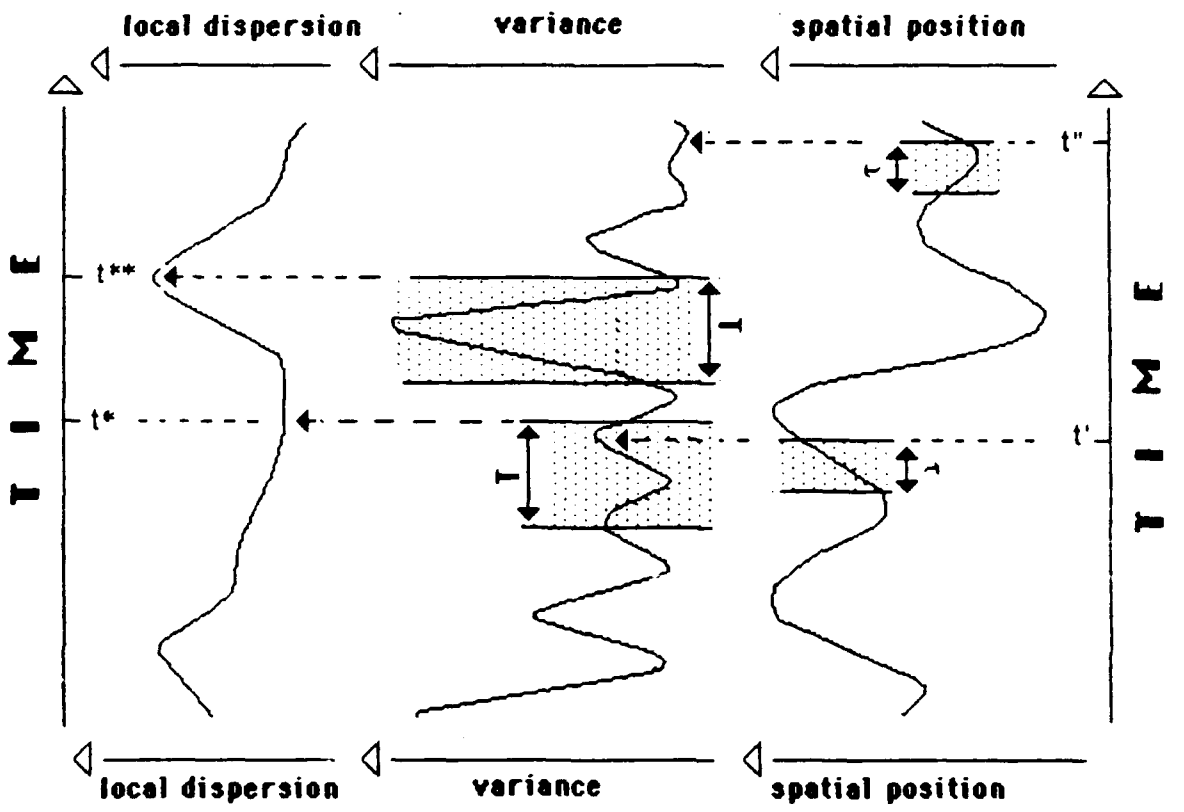
local dispersion
variance
spatial position
TIME
t**
t*
t"
t'
T
T
τ
τ
local dispersion
variance
spatial position
TIME

FIGURE 2

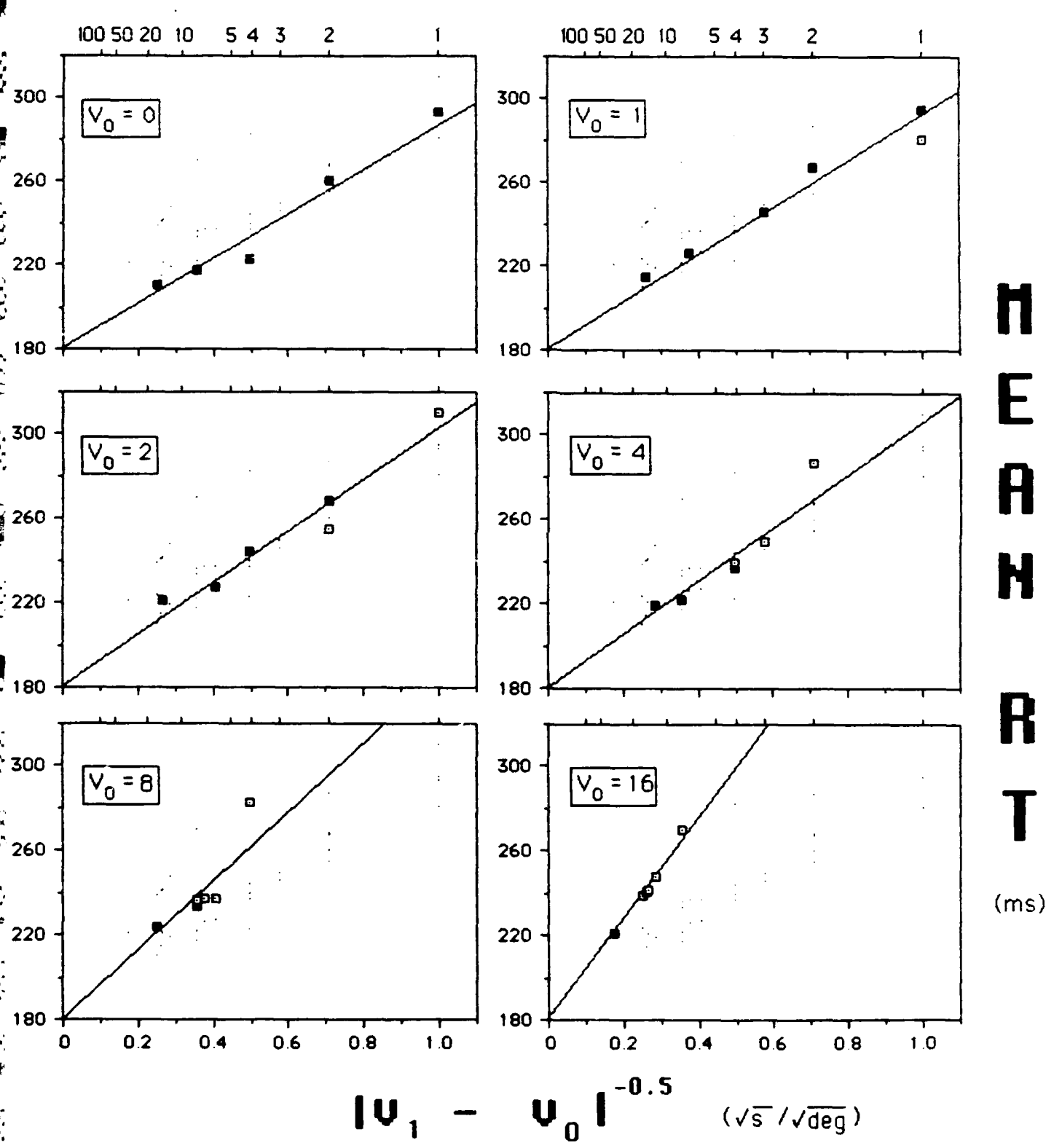
$|V_1 - V_0|$ (deg/s)
100 50 20 10 5 4 3 2 1
$V_0 = 0$
$V_0 = 1$
$V_0 = 2$
$V_0 = 4$
$V_0 = 8$
$V_0 = 16$
300
260
220
180
0 0.2 0.4 0.6 0.8 1.0
$|V_1 - V_0|^{-0.5}$ ($\sqrt{s}$ / $\sqrt{deg}$)
MEAN RT (ms)

FIGURE 3

AD-A193 076 PERCEPTION OF MOTION IN STATISTICALLY-DEFINED DISPLAYS 2/2
(U) NORTHWESTERN UNIV EVANSTON IL CRESAP NEUROSCIENCE
LAB R SEKULER 15 FEB 88 AFOSR-TR-88-0288 AFOSR-85-0370
UNCLASSIFIED F/G 5/8 NL

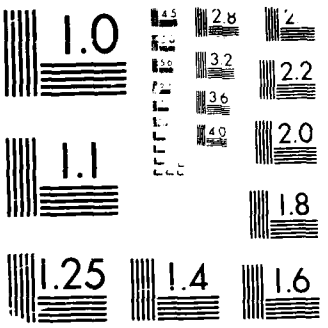

MICROCOPY RESOLUTION TEST CHART

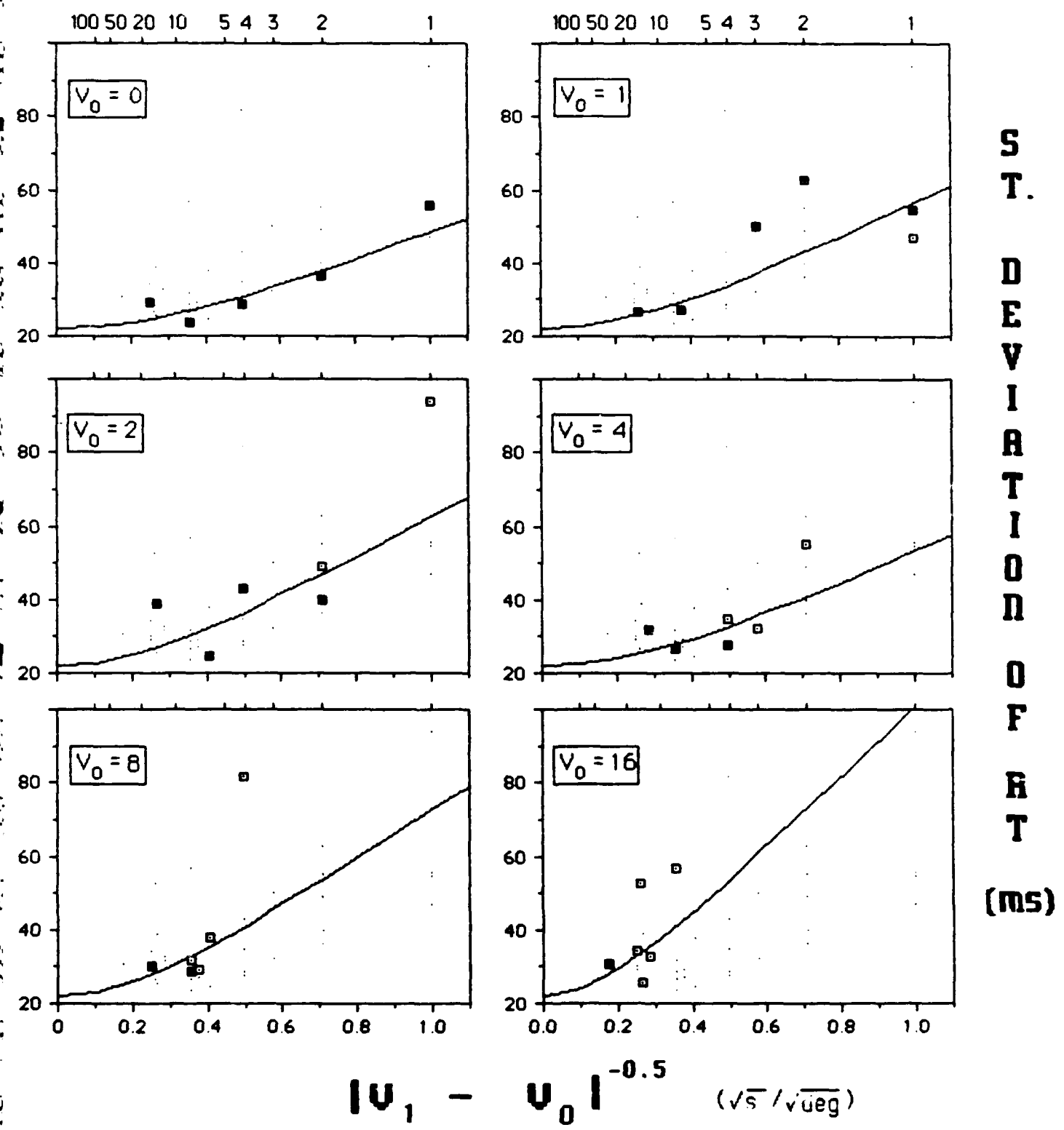
$|V_1 - V_0|$ (deg/s)
100 50 20 10 5 4 3 2 1
$V_0 = 0$
$V_0 = 1$
$V_0 = 2$
$V_0 = 4$
$V_0 = 8$
$V_0 = 16$
80
60
40
20
0 0.2 0.4 0.6 0.8 1.0
0.0 0.2 0.4 0.6 0.8 1.0
ST. DEVIATION OF RT (ms)
$|V_1 - V_0|^{-0.5}$ ($\sqrt{s}$ / $\sqrt{deg}$)

FIGURE 4

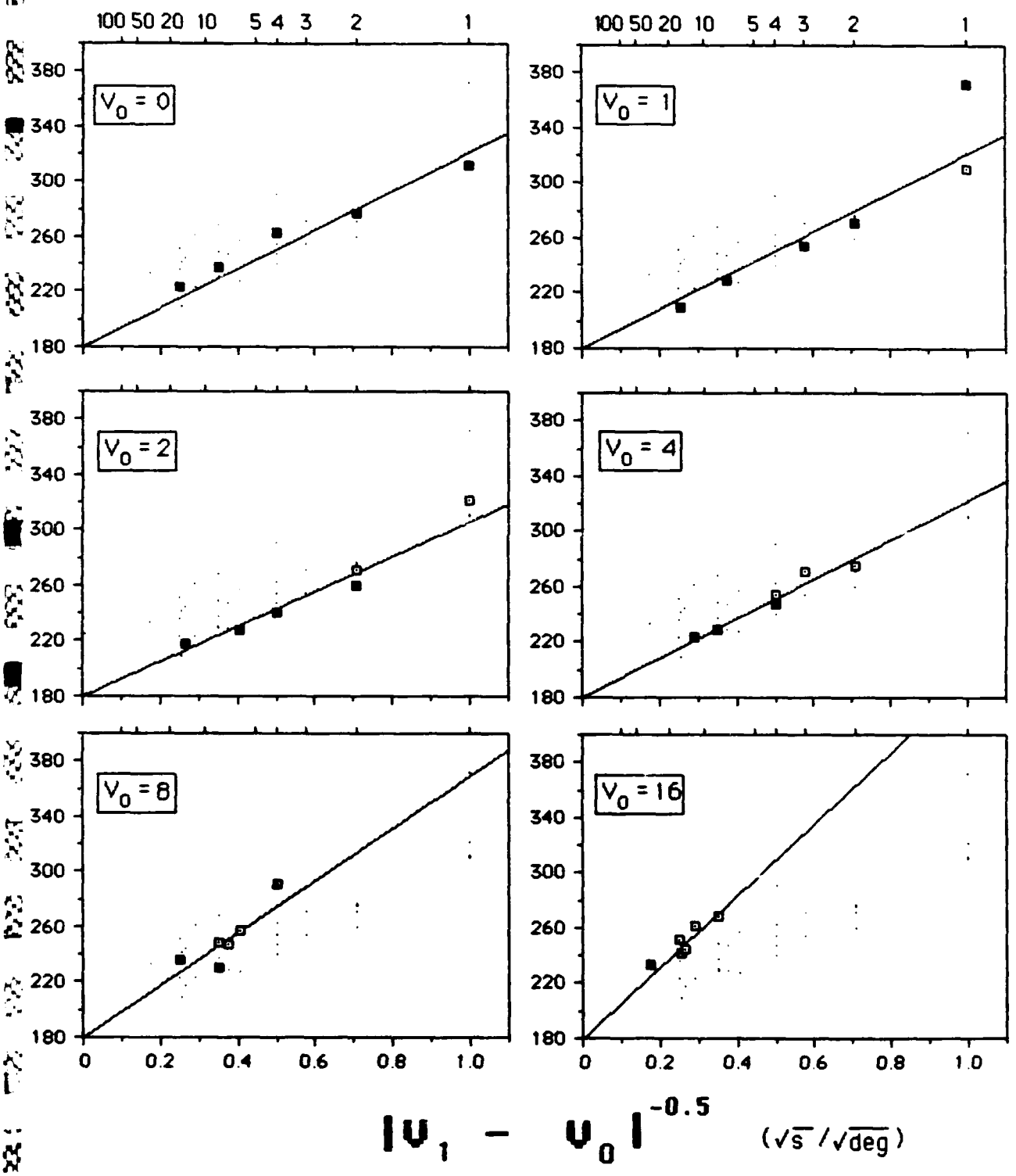
|V1 − V0| (deg/s)
100 50 20 10 5 4 3 2 1
V0 = 0
V0 = 1
V0 = 2
V0 = 4
V0 = 8
V0 = 16
380
340
300
260
220
180
0 0.2 0.4 0.6 0.8 1.0
|V1 − V0|^-0.5 (√s / √deg)
MEAN RT
(ms)

FIGURE 5

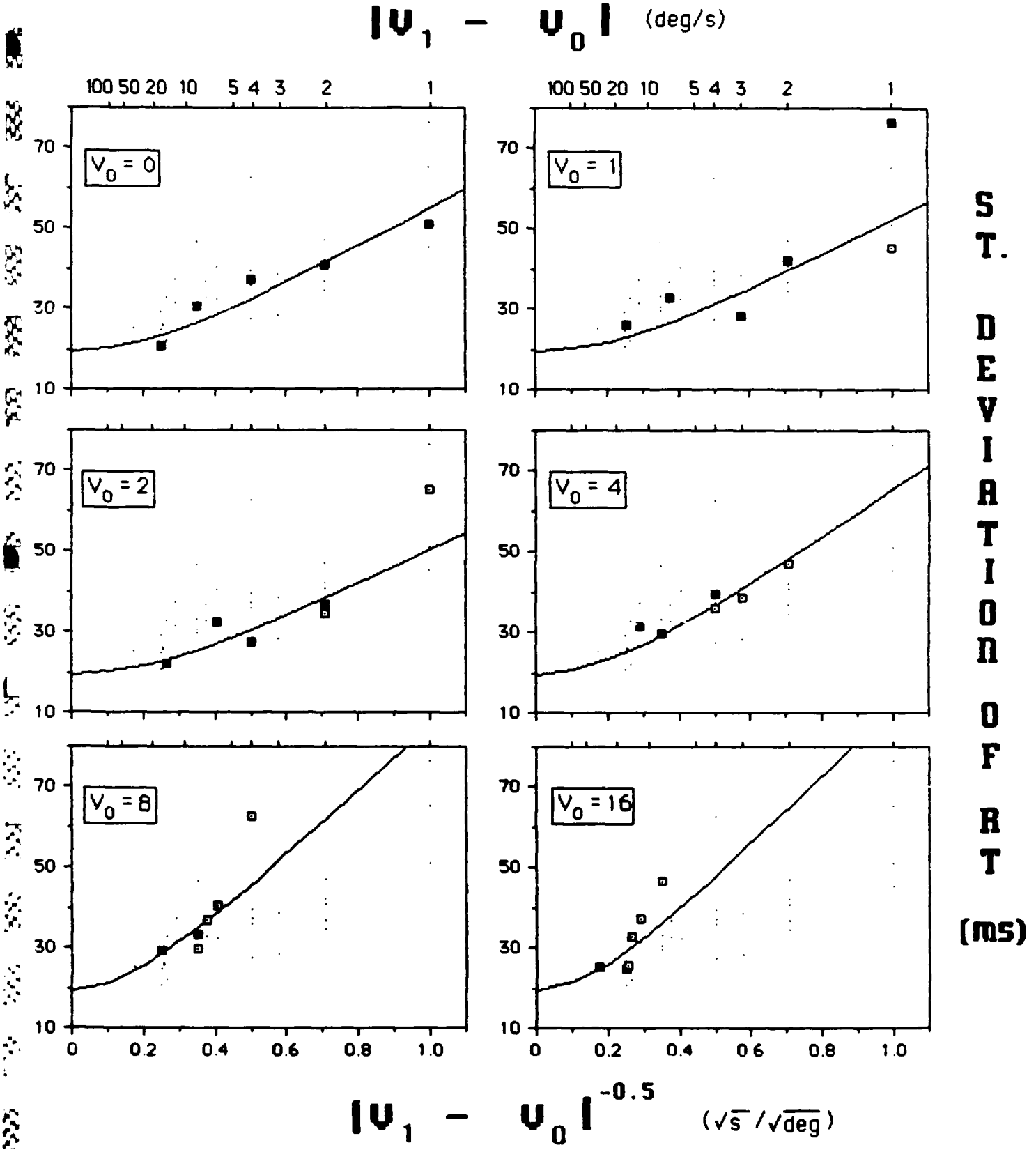
|V1 − V0| (deg/s)
100 50 20 10 5 4 3 2 1
V0 = 0
V0 = 1
V0 = 2
V0 = 4
V0 = 8
V0 = 16
70
50
30
10
0 0.2 0.4 0.6 0.8 1.0
ST. DEVIATION OF RT (ms)
|V1 − V0|^-0.5 (√s / √deg)

FIGURE 6

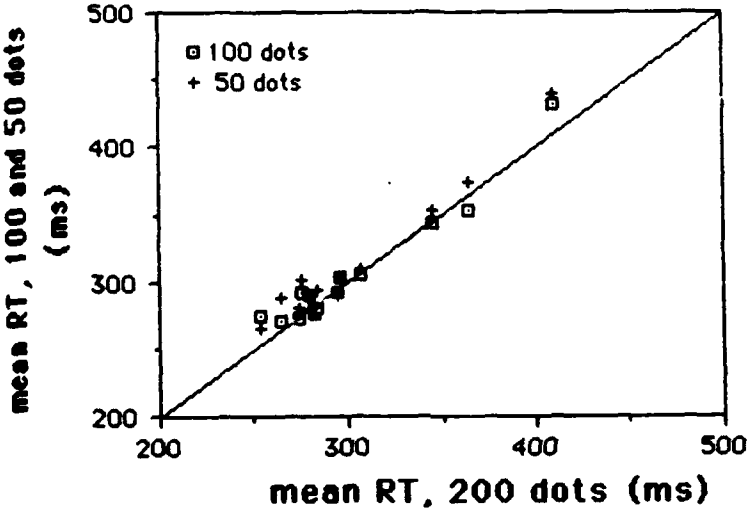
500
400
300
200
200
300
400
500
100 dots
50 dots
mean RT, 100 and 50 dots (ms)
mean RT, 200 dots (ms)

FIGURE 7

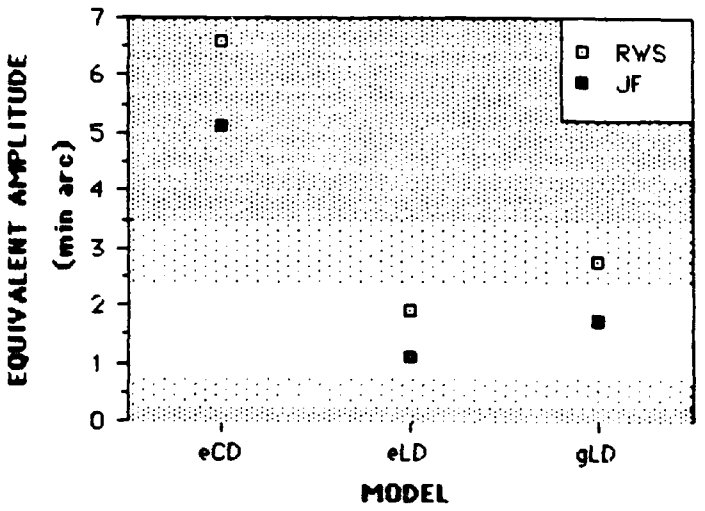
EQUIVALENT AMPLITUDE
(min arc)
7
6
5
4
3
2
1
0
RWS
JF
eCD
eLD
gLD
MODEL

FIGURE 8

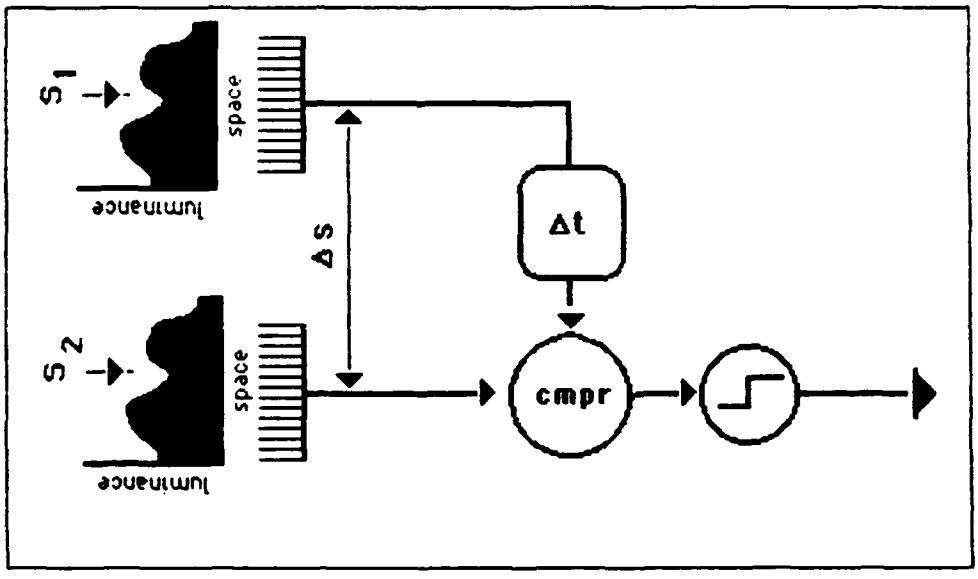

FIGURE 9

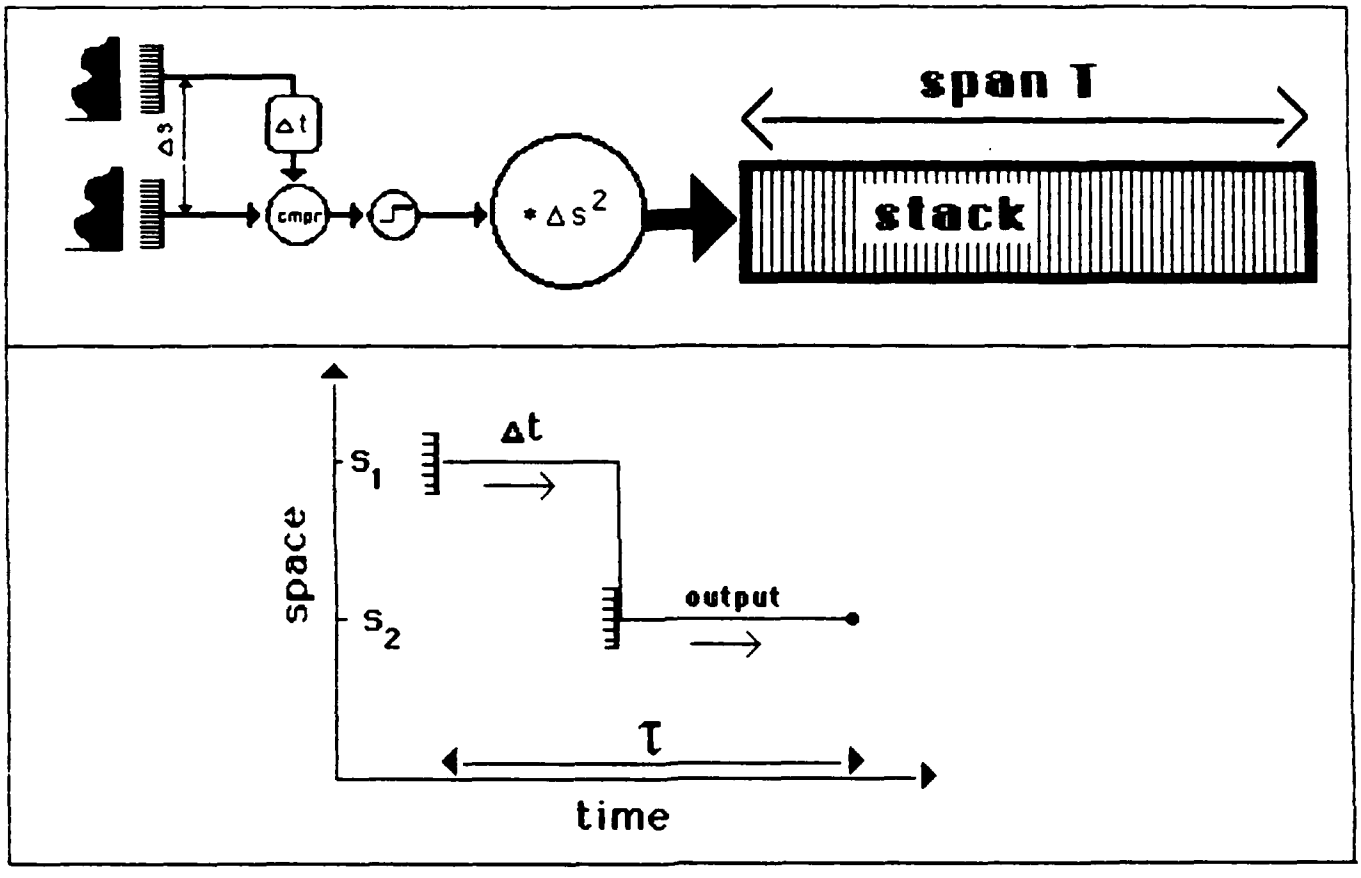

FIGURE 10

END

DATE

FILMED

DTIC

JULY 88